Casarin, Roberto; Costola, Michele; Yenerdag, Erdem

Working Paper

Financial bridges and network communities

SAFE Working Paper, No. 208

Provided in Cooperation with:
Leibniz Institute for Financial Research SAFE

Suggested Citation: Casarin, Roberto; Costola, Michele; Yenerdag, Erdem (2018) : Financial bridges and network communities, SAFE Working Paper, No. 208, Goethe University Frankfurt, SAFE - Sustainable Architecture for Finance in Europe, Frankfurt a. M., https://doi.org/10.2139/ssrn.3178053

This Version is available at:
https://hdl.handle.net/10419/203318

HOUSE OF FINANCE
WORKING PAPER SERIES

Roberto Casarin – Michele Costola – Erdem Yenerdag

Financial Bridges and Network Communities

SAFE Working Paper No. 208

SAFE | Sustainable Architecture for Finance in Europe
A cooperation of the Center for Financial Studies and Goethe University Frankfurt

House of Finance | Goethe University
Theodor-W.-Adorno-Platz 3 | 60323 Frankfurt am Main

Tel. +49 69 798 30080 | Fax +49 69 798 33910
info@safe-frankfurt.de | www.safe-frankfurt.de

Non-Technical Summary

Financial crises and systemic risks proved to play central roles as shock transmitters to the real economy, threatening the stability of the economic and financial systems. These phenomena have boosted a massive interest in the literature which deeply investigated systemic risk and contagion channels on the financial systems.

Generally, systemic risk may arise as the interactions among financial institutions and markets which, consequently, lead to financial crises. A stylized fact that occurs often in real networks is the presence of a group of nodes which share common properties or play a similar role within the network. These community structures have been recognized also in finance with the presence of key nodes (community bridges) linked through short-cuts to otherwise separated communities. The case in point to better understand the role of the community structure in a network is provided by epidemiology. A parallelism with the financial stability indicates that the mitigation and prevention of the spread in infectious diseases (financial contagion) can be attained by seeking actively to immunize the super-spreaders. However, the presence of a community structure significantly affects the dynamic of the disease: immunization interventions focusing on nodes strongly linked with other communities (community bridges) are in this case more effective than the ones which aim to the highly connected nodes in the whole network. The reason is that community bridges are more relevant in spreading out contagion with respect to the nodes with fewer inter-community connections in the group: with the latter, contagion may stop before spreading out to the other communities. Hence, in a network with a community structure, classical connectedness measures can lead to the misidentification of a given SIFI at least in two cases: i) a financial institution shows a lower total degree with respect to the other nodes in the community, but a higher degree to the nodes belonging to other communities (false negative); ii) a financial institution shows a higher total degree with respect to the other nodes in the community, but a lower degree to the nodes belonging to other communities (false positive). Therefore, also in a financial network, the node immunization through the identification of highly connected nodes may not be effective in a network with community structure.

On this ground, the aim of this paper is to investigate the topology of the financial networks focusing on the detection of financial communities and community bridges to overcome the weakness of classical connectedness measure. We denote these communities as the Systemically Important Financial Communities (SIFC) defined as a group of nodes that belong to the community with the highest inter-connectivity density of the network. In this regard, we propose measures of connectedness to describe the inter- and intra community connectivity in financial networks. In the empirical analysis, we investigate the European financial system from 1996 to 2013 including all the financial firms (active and dead). Findings show a time-varying com-munity structure in the European financial networks which exhibits an increasing number of communities during periods of financial distress. By analyzing the global financial crisis and European sovereign debt crisis, our results show that the network exhibits a structure with the presence of a core block (the SIFC) acting as the shock spreader to a second block, the receiver. In both periods, insurances play a primary role in spreading shocks with respect to other financial sectors (i.e. banks). In fact, the SIFC contains a share of insurances which is more than the half of the total market and the largest financial institutions in terms of market capitalization.

Financial Bridges and Network Communities*

Roberto Casarin† Michele Costola‡ Erdem Yenerdag§

This version: September 29, 2018

Abstract

We analyze the global financial crisis and the European sovereign debt crisis showing that the European network exhibits a strong community structure with two main blocks acting as shock spreader and receiver, respectively. We provide evidence of the prominent role played by insurances in the spread of systemic risk in both crises and demonstrate that institutions with a large number of inter-community linkages (community bridges) are more relevant in spreading contagion than institutions with large centrality. Network measures based on the community structure can provide a better description of the financial connectedness and effective early warning indicators for financial losses.

Keywords: Systemic Risk; Financial Institutions; Network Communities; Financial Crises
JEL Classification: G12; G29; C51

*We thank Ana Babus, Monica Billio, Francis Bloch, Fulvio Corsi, Philip H. Dybvig, Christian Kubitza, SangMok Lee, Gianni De Nicoló, Lorenzo Frattarolo, Mark Hallam, Manfred Kremer, Loriana Pelizzon, Tuomas A. Peltonen, Brian Rogers and the participants at the EARLINESS.eu Workshop (SAFE, Goethe University Frankfurt), the Internal Macro Seminars (Washington University in St. Louis), the Domenico Econometric Workshop 2017 (Ca' Foscari University of Venice, Italy), CREDIT Conference 2017 (Ca' Foscari University of Venice, Italy), SAFE Annual Meeting 2017 (Goethe University, Frankfurt am Main, Germany), EFiC 2017 (University of Essex, Colchester, UK) and CFE 2016 Meeting (Siville, Spain). Michele Costola acknowledges financial support from the Marie Skłodowska-Curie Actions, European Union, Seventh Framework Program HORIZON 2020 under REA grant agreement n. 707070. He also gratefully acknowledges research support from the Research Center SAFE, funded by the State of Hessen initiative for research LOEWE.
†Department of Economics, Ca' Foscari University of Venice, Dorsoduro 3246, 30123 Venice (Italy), r.casarin@unive.it (e-mail).
‡SAFE, House of Finance, Goethe University Frankfurt, Theodor-W.-Adorno-Platz 3, 60323 Frankfurt am Main (Germany), costola@safe.uni-frankfurt.de (e-mail). (corresponding author)
§Department of Economics, Washington University in St. Louis, One Brookings Drive Campus Box 1208, Saint Louis, MO 63130 (USA) erdemyenerdag@wustl.edu (e-mail).

1 Introduction

Financial crises and systemic risk proved to play a central role as shock transmitters to the real economy, threatening the stability of the economic and financial systems (i.e., Allen et al., 2012; Giglio et al., 2016). These phenomena attracted increasing interest in the literature which deeply investigated systemic risks and contagion channels in the financial system (Billio et al., 2012; Brownlees and Engle, 2017; Tobias and Brunnermeier, 2016). Usually, systemic risks arise from the interactions between financial institutions and the market which eventually, might lead to financial crises (Allen and Carletti, 2013).

Network models represent an efficient way to describe financial relationships between financial institutions: the analysis of linkages allows to monitor the structure of the system in order to pursue financial stability (Diebold and Yilmaz, 2015; Scott, 2016).[1] Highly interconnected financial networks can be "robust-yet-fragile". The connectedness acts as a shock absorber for a given range, while beyond that range, it becomes a "shock-propagator mechanism" where robustness turns to fragility by generating systemic risks (Haldane, 2013). Indeed, the characteristics that make a financial network more resilient are the same that, under different conditions, bring instability to the financial system (Acemoglu et al., 2015). To enhance the resilience of the financial system and mitigate systemic risk, policymakers aim to identify the so-called Systemically Important Financial Institutions (SIFIs) (Freixas et al., 2000; Thomson, 2010).

With the studies of financial network topologies, different indicators have been proposed to measure systemic risk: global measures to describe the structure of financial networks (e.g., density and assortativity) and local measures to detect SIFIs (e.g., degree and centrality).

A stylized fact which often occurs in networks is that the probability of having an edge between a pair of vertices is not equal across all possible pairs. Different than pure random graphs, real-world networks display heterogeneity not only globally, but also locally with a high concentration of edges within groups of nodes and low concentrations between groups. This phenomenon is known as community structure or network modularity (Leicht and Newman, 2008; Newman, 2018) where a community is defined as a group of nodes which share common properties or play a similar role within the network (Fortunato, 2010).

Community structures have also been recognized in financial networks with the presence of nodes linked through short-cuts to otherwise separated communities (Haldane, 2013). These key-nodes act as community bridges. These structures have not been fully investigated in the

[1] The Financial Stability Board considers interconnectedness a key criteria to identify the systemic importance of the financial institutions (Financial Stability Board, 2009).

financial literature. Notable exceptions are represented by de Souza et al. (2016), Puliga et al. (2016) and Bargigli and Gallegati (2013).[2]

A case in point to better understand the role of the community structure in a network is provided by epidemiology. Parallelism with the financial stability indicates that the mitigation and prevention of the spread in infectious diseases (financial contagion) can be attained by seeking actively to immunize the super-spreaders (Haldane and May, 2011). However, the presence of a community structure significantly affects the dynamic of the disease: immunization interventions focusing on nodes strongly linked with other communities (community bridges) are in this case more effective than the ones which aim to the highly connected nodes in the whole network (Salathé and Jones, 2010). The reason is that community bridges are more relevant in spreading out contagion with respect to the nodes with fewer inter-community connections in the group: with the latter, contagion may stop before spreading out to the other communities.

More generally, a critical aspect of node centrality measures is their sensitivity to the degree heterogeneity. In the presence of strong degree heterogeneity, e.g., hubs and core-periphery structures, most of the components have null centrality. Hence, in a network with a community structure, classical connectedness measures can lead to the misidentification of a SIFI at least in two cases: i) a financial institution shows a lower total degree with respect to the other nodes in the community, but a higher degree to the nodes belonging to other communities (false negative) and ii) a financial institution shows a higher total degree with respect to the other nodes in the community, but a lower degree to the nodes belonging to other communities (false positive). Therefore, also in a financial network, the node immunization through the identification of highly connected nodes may not be effective in a network with community structure (Karrer and Newman, 2011).

On this ground, the paper aims to investigate the topology of financial networks focusing on the detection of financial communities and community bridges to overcome the weakness of classical connectedness measure. We denote these communities as the Systemically Important Financial Communities (SIFCs) defined as a group of nodes that belong to the community with the highest inter-connectivity density of the network. In this regard, we propose measures of connectedness to describe the inter- and intra community connectivity in financial networks. We identify the communities by applying a Weighted Stochastic Block Model (WSBM) which

[2]Bargigli and Gallegati (2013) investigate credit communities on a Japanese bank-firm weighted and directed bipartite network finding a strengthening of Japanese communities over time. Puliga et al. (2016) provide evidence through an accounting network that regional bank communities change weakening geographically boundaries. Finally, de Souza et al. (2016) identify Brazilian banking communities through inter-banking exposures showing that a large part of them include non-large banks.

considers both the edge existence and the edge weight of the network (Aicher et al., 2014). The model allows to have a compact characterization of the network structure through blocks and represents a generalization of the Stochastic Block model (SBM) introduced by Holland et al. (1983). Hałaj and Kok (2013) show that SBM can be successfully used to simulate contagion and cascades since it allows to circumvent the bias problem in standard random network models which tend to underestimate tails and contagion risk. To our knowledge, this paper is the first to introduce this approach in the financial economics literature.

In the empirical analysis, we investigate the European financial system from 1996 to 2013 including all the financial firms (active and dead). Dynamic networks of European financial institutions are inferred through Granger-causality tests using a rolling window estimation as performed in Billio et al. (2012). This bivariate approach for network estimation allows to easily deal with large datasets and delisting in stocks markets avoiding the survivorship bias (Shumway, 1997). The WSBM model is independent by the chosen methodology in the network estimation, and alternative techniques such as graph-based approaches and sparse models can be applied (i.e., Ahelegbey et al., 2016a,b; Hautsch et al., 2015).

Our findings show that there exist a time-varying community structure in the European financial network which exhibits an increasing number of communities during periods of financial distress. An increase of the number of communities is a signal of network complexity, which may reflect into heterogeneous connectivity patterns and shock propagation mechanisms among financial institutions. Using the new proposed community connectivity measures, we find that the density of the financial network is mainly driven by the inter-linkages. This highlights the primary role played by financial community bridges in the spread of shocks across the communities and consequently, to the whole network. We show that these measures represent a better early warning indicator in terms of future financial losses with respect to the classical connectedness measures.

Moreover, we analyze the European network during the global financial crisis and the European sovereign debt crisis and show that its community structure exhibits a SIFC acting as the shock spreader to a second block, the receiver. In both periods, we find that insurances play a prominent role in spreading shocks with respect to other financial sectors (i.e., banks). In fact, the SIFC contains a share of insurances which is more than the half of the total market and include the largest financial institutions in terms of market value. The key reason is due to the fact that the insurance industry is no longer mainly involved in the traditional business model where risk is well diversified and relies on insurance policies (Baranoff and Sager, 2009;

Brewer et al., 2007). Insurances are now exposed to macroeconomic and non-diversifiable factors (Acharya et al., 2011) resulting from investment decisions (i.e., fixed income linked life insurance policies with minimum guarantees). Hence, firm characteristics such as size, leverage, assets' riskiness, and liquidity mismatch represent the conditions that turn banks as well as insurances into SIFIs (Acharya et al., 2016). Furthermore, regulatory constraints on insurances contribute to fire sales in the corporate bond market which in turn entail systemic risk and other significant externalities in the financial markets (Ellul et al., 2011; Shleifer and Vishny, 2011).

The remainder of the paper is organized as follows. Section 2 discusses network community structures and propose connectivity measures. Section 3 presents the empirical analysis of the European financial system while Section 4 shows the ability of community connectivity measures in predicting financial losses and their impact on the European financial network in terms of contagion. Finally, Section 5 concludes.

2 Community Connectivity Measures

2.1 A Community Generative Model

Network models represent a useful tool to depict financial systems given their high degree of interdependence (Franklin Allen, 2009). In financial networks, a node represents a financial institution (e.g., a bank or an insurance company) and an edge has the interpretation of financial linkage between to institutions. In mathematical terms, a network can be represented through the notion of the random graph given by a set of nodes and a set of parameters driving the probability of the existence of an edge between all pairs of nodes. Often, real-world networks have structures which are not fully observable due to missing or unavailable information Jackson (2010). For instance, socio-economic conditions (i.e., level of income) can represent one of the drivers which lead to the formation of different political groups (clusters) in social networks. In financial networks, latent structures can be driven by portfolio exposures to different financial and macroeconomic risk factors which can lead to heterogeneous interdependence among financial institutions. Cifuentes et al. (2005) propose a model where financial institutions are linked through portfolio holdings and show that contagion is mostly driven by changes in asset prices. Caccioli et al. (2014) show that not only common asset holdings but also extreme portfolio diversification can create systemic risk worsening financial contagion in the network. As observed in Franklin Allen (2009), financial network structures respond differently to the propagation of shocks (contagion), and consequently, the resilience of the whole system also depends on the

position in the network of the institution affected by the shock. Clearly, revealing these latent structures can provide valuable information for a better comprehension of the financial system concerning propagation of shocks and hence, connectivity.

The Stochastic Block Model (SBM) is one of the most flexible generative models for random networks since it allows for different types of connectivity structures while preserving parameter parsimony. In an SBM of n nodes, each node is assigned randomly to one of the K groups of nodes called communities or blocks. The label z_i with values in $1, \ldots, K$ indicates the block to which the node i is assigned. The variable a_{ij} takes value 1 if an edge exists between node i and j and 0, otherwise. The probability of an edge between nodes i and j depends on their community labels z_i and z_j, that is,

$$P(a_{ij} = 1) = \theta_{z_i z_j}, \tag{1}$$

where $0 \leq \theta_{lk} \leq 1$ and $l, k = 1, \ldots, K$ are the elements of the so-called affinity matrix which describes the connectivity between the communities. Depending on the ranking between the elements of the affinity matrix, the network has different connectivity structure between nodes (institutions) in the same community (intra-community connectivity) and between nodes of different communities (inter-community connectivity).

In the following, we define four structures which typically emerge in real-world networks and are useful for interpreting the results of our empirical analysis. We refer to an assortative structure when intra-community linkage intensity is larger than the inter-community one (i.e, $\theta_{ii} > \theta_{ij}$ with $i \neq j$). Conversely, a disassortative structure appears when intra-community linkage intensity is smaller than the inter-community one (i.e, $\theta_{ii} < \theta_{ij}$ with $i \neq j$). To exemplify, Panel (a) and (b) (Figure 1) provide an example of the assortativity and disassortativity, respectively, in a network with four communities.

Differently, when $\theta_{ii} > \theta_{jj}$ and $\theta_{ij} > \theta_{jj}$ for all $i \neq j$, linkages are most likely to be in one community (core) and nodes in other communities (periphery) are more likely connected to those in the core than to each other. We refer to this structure as core-periphery[3].

Finally, an ordered structure arises when the connectivity of each community follows a chain and the nodes of one community are connected to nodes of at the most two other communities, that is, $\theta_{ij} > 0$ if $j = i + 1, i - 1$ and $\theta_{ij} = 0$ otherwise, for all $i \neq j$ (see Panel(d)). In Appendix A, we include a full description of the stochastic block model. Moreover, we propose

[3]See Panel(c), for example.

a new dynamic specification and the inference procedure used in the empirical analysis.

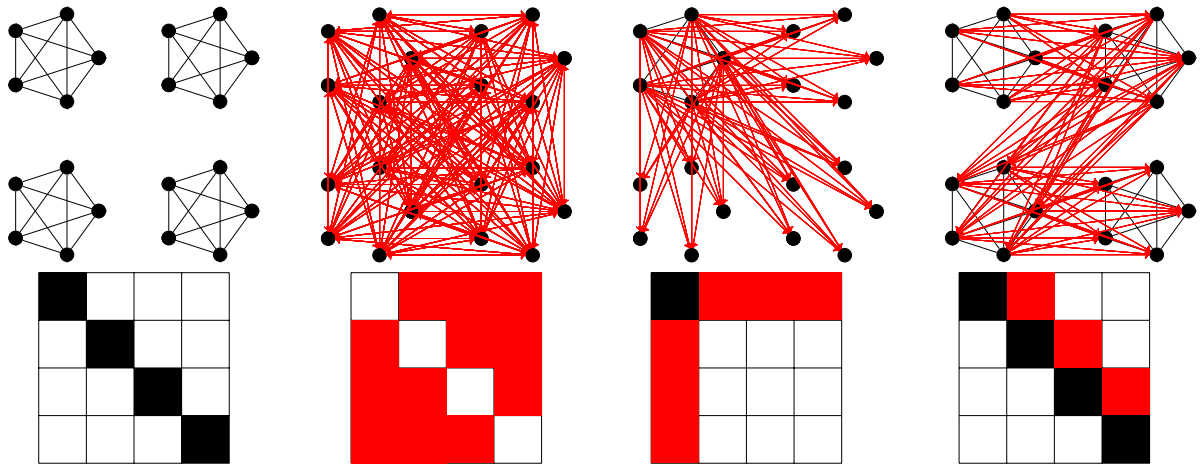

(a) Assortative (b) Disassortative (c) Core-Periphery (d) Ordered

Figure 1: Examples of potential community connectivity patterns as in Aicher et al. (2014). The first (second) row reports the graph (adjacency matrix) of the network ordered by community membership of the nodes. Black (red) color indicates intra (inter) linkages: (a) Assortative type shows mainly intra-linkages within community; (b) Disassortative type shows inter-linkages in between communities; (c) Core-Periphery type shows the presence of a core with intra- and inter-linkages to the periphery (the other communities) which is in turn mainly connected to the core and (d) Ordered type shows inter-linkages and intra-linkages from the top to the bottom.

2.2 Connectivity Measures

As in the previous section, let $z_{it} \in \{1, \dots, K_t\}$ be the allocation variable indicating the community to which the institution i belongs to at time t, K_t the number of communities, n_{kt} the number of institutions in the k-th community, and n_t the number of institutions in the network at time t.

The in- and out-degree of a node i that are given by

$$d_{it}^{+} = \sum_{j=1}^{n_t} A_{ji,t}, \quad d_{it}^{-} = \sum_{j=1}^{n_t} A_{ij,t}, \tag{2}$$

respectively, and can be decomposed as follows

$$\begin{aligned} d_{it}^{+} &= d_{it}^{+,INTRA} + d_{it}^{+,INTER}, \\ d_{it}^{-} &= d_{it}^{-,INTRA} + d_{it}^{-,INTER}. \end{aligned} \tag{3}$$

The intra- and inter-community degrees, in Equation 3, are given by

$$\begin{aligned} d_{it}^{+,INTRA} &= \sum_{j=1}^{n_t} A_{ji,t}\mathbb{I}(z_{it} = z_{jt}), \quad d_{it}^{+,INTER} = \sum_{j=1}^{n_t} A_{ji,t}(1 - \mathbb{I}(z_{it} = z_{jt})), \\ d_{it}^{-,INTRA} &= \sum_{j=1}^{n_t} A_{ij,t}\mathbb{I}(z_{it} = z_{jt}), \quad d_{it}^{-,INTER} = \sum_{j=1}^{n_t} A_{ij,t}(1 - \mathbb{I}(z_{it} = z_{jt})). \end{aligned} \tag{4}$$

The intra- and inter-community degrees measure the connectivity of node (institution) i with the other nodes (institutions) in the same community (INTRA) and with the nodes of the other communities (INTER). The out (in) inter-linkages allows to identify which nodes play the role of financial bridges as shock spreaders (receivers) to (from) other communities. In particular, the inter-linkages among a given community to another one can be viewed as a sub-bipartite network.

Hence, the density of the network is given by

$$f_t = \frac{1}{2n_t(n_t - 1)} \sum_{i=1}^{n_t} (d_{it}^{+} + d_{it}^{-}), \tag{5}$$

which also can be represented as the convex combination of intra- and inter-community densities as follows

$$f_t = w_{1t} f_t^{INTRA} + w_{2t} f_t^{INTER}. \tag{6}$$

Moreover, the densities are defined as

$$f_t^{INTRA} = \frac{1}{2c_{1t}} \sum_{i=1}^{n_t} (d_{it}^{+,INTRA} + d_{it}^{-,INTRA}), \quad f_t^{INTER} = \frac{1}{2c_{2t}} \sum_{i=1}^{n_t} (d_{it}^{+,INTER} + d_{it}^{-,INTER}), \tag{7}$$

where f_t^{INTRA} is equal to 1 if all the community sub-networks are complete graphs and analogously, f_t^{INTER} is equal to 1 if all the inter-community sub-networks are complete graphs. If there is no edges between the communities, i.e., $f_t^{INTER} = 0$, then there is no risk of spreading contagion from one community to another. In this case, each community can be viewed as a separated network and the identification of the SIFIs reduces to find central institutions within each community as in standard connectedness measures (Billio et al., 2012; Diebold and Yılmaz, 2014; Diebold and Yilmaz, 2015).

The normalizing constants, c_{1t} and c_{2t} , given in Equation 7, provide the total degree of the sub-networks when the corresponding graphs are complete, and they are defined by the following

equations

$$c_{1t} = \sum_{k=1}^{K_t} n_{kt}(n_{kt} - 1), \quad c_{2t} = \sum_{k=1}^{K_t} \sum_{l \neq k} n_{kt} n_{lt}. \tag{8}$$

The weights, w_{1t} and w_{2t}, in Equation 6, are given by

$$w_{1t} = \frac{1}{n_t(n_t - 1)} c_{1t}, \quad w_{2t} = \frac{1}{n_t(n_t - 1)} c_{2t}. \tag{9}$$

They are functions of the number of nodes in each community and satisfy $w_{1t} + w_{2t} = 1$, $\forall t$.

By increasing the number of communities K_t, the importance of the inter-community density increases (see red line in the left plot of Figure 2). For $K_t > 2$ the inter-community density is more relevant than the intra-community in the whole connectivity of the network. We also study the effect of the distribution of the community sizes on the contribution of the inter-community density to the network density and find that (see right plot of Figure 2):

- a Dirac distribution, corresponds to the case of communities of equal size (solid);
- a uniform distribution, represents the case all community sizes are equally represented in the network (dashed);
- a symmetric beta distributed community size, implies a community with a large size and then various communities with smaller size (dotted).

Comparing the different lines (solid, dashed and dotted) in the left plot of Figure 2, one can see that for $K_t > 2$ the largest weight for the inter-community density is associated to the uniform distribution.

3 Empirical Analysis

We analyze the European financial market and its community structure during the period of 1996-2013 considering the model and community connectivity measures presented in Section 2.[4] We discuss the community structure of the network on two specific moments: the Global financial crisis and the European sovereign debt crisis. Finally, we perform an immunization exercise on the European financial network during the European sovereign debt crisis showing that removing the institutions with highest inter-community degrees is more effective than the ones with the highest inter out community degrees.

[4]Further details on the estimation of the optimal number of blocks and the model selection according α are reported in Appendix B.

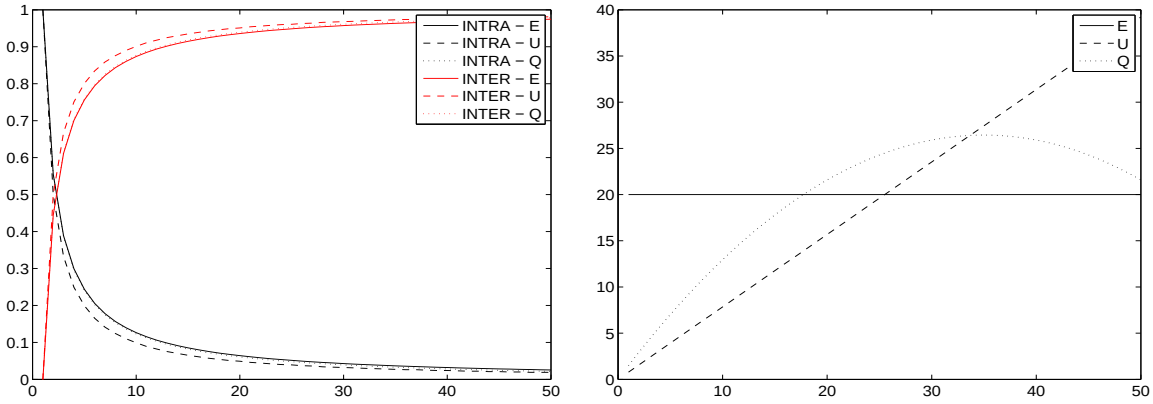

Figure 2: Intra- and inter-community densities (red and black lines, respectively, left plot) and number of nodes n_{kt} (right plot) per community $k = 1, \ldots, 50$ (horizontal axis), assuming a Dirac's distribution, $n_{kt} \propto n_t/K_t$ (solid lines), a uniform distribution, $n_{kt} \propto n_t k$ (dashed lines) and translated symmetric beta distribution, $n_{kt} \propto n_t(70-k)k$ (dotted lines).

3.1 Data Description

The dataset is composed of the daily closing price series at a daily frequency from 29^{th} December 1995 to 16^{th} January 2013. To cope with survivorship bias (Shumway, 1997), we include all European financial institutions active and dead. Financial institutions are classified under the Industry Classification Benchmark (ICB) which comprises four industry levels. The financial industry is represented at the first level by the class 8000. We consider its four super-sectors (second level):[5] i) Banks (code 8300); ii) Insurance (code 8500); iii) Real Estate (code 8600) and iv) Financial Services (code 8700).

The built database is suitable to represent the European financial systems since it covers a total of 766 European financial firms[6] traded in the largest European financial markets (core and peripheral). The markets with the number of institutions in round brackets are: Austria (15), Belgium (30), France (81), Germany (136), Greece (56), Ireland (5), Italy (95), Netherlands (4), Spain (40) and United Kingdom (304).

We estimate dynamic networks of European financial institutions through Granger-causality tests (Billio et al., 2012) on daily returns using a rolling window approach with a length of 252 observations (approximately 1 year) and obtain a total of 4197 adjacency matrices. [7]

[5] See the ICB's website: `www.icbenchmark.com`. The Industry Classification Benchmark document with Structure and Definitions for the type of Industry (Financials Industry at Section 7.9) is available at `http://www.ftse.com/products/downloads/ICB_Rules.pdf`.

[6] Data have been downloaded from Datastream® using Thomson Reuters Worldscope lists®. The complete list is available upon request to the authors.

[7] The estimations have been parallelized and implemented in Matlab on the SCSCF (Sistema di Calcolo Scientifico Ca' Foscari) cluster multiprocessor system which consists of 4 nodes; each comprises four Xeon E5-4610 v2 2.3GHz CPUs, with 8 cores, 256GB ECC PC3-12800R RAM, Ethernet 10Gbit, 20TB hard disk system with Linux.

3.2 Community Structure and Financial Bridges

In the presented framework, a community structure would indicate the existence of distinct groups of nodes playing a different role in the network connectivity. It is worth noting that the definition of community or block here is more general with respect to the usual assortativity based definition where edges primarily exist within groups.

In a network with no community structure (e.g., one community), all financial institutions show an homogeneous connectivity level and thus, a shock would hit all the system in the same manner. Clearly, this does not imply the absence of systemic risk. Having the same patterns of connectivity between the nodes, the robust-yet-fragile property could lead to a resilient network when shocks are in a given range and into a fragile one when shocks are above that range.

Consequently, a strengthening in the community structure leads to a disintegration of the financial network in many sub-networks where each block of institutions plays a different role in terms of connectedness within and without the group. Different community connectivity patterns form the network structure which is one (or a mixture) of the types defined in Section 2.1 and represented in Figure 1.

Given these premises, we analyze the community structure of the European financial network along with the CISS (Hollo et al., 2012) as reported in Figure 3. The CISS is a composite indicator of contemporaneous stress in the financial system released periodically by the European Central Bank (ECB). As any classical financial stress indicator, it is useful in monitoring the current level of distress in the financial system.

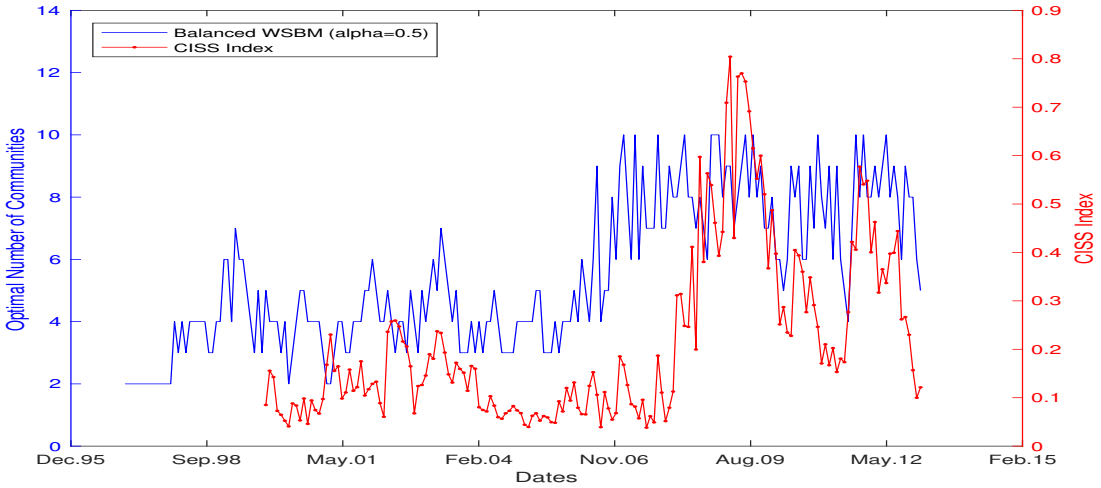

Figure 3: The number of communities K (black solid line) and the CISS indicator (red dashed line) by Hollo et al. (2012) during 1996-2013.

The two series exhibit a significant and positive Spearman's correlation equal to 0.61 indicating that during financial stress periods a strengthening of the structure is likely to be expected.[8] We report in Figure 4 the size of the communities (shaded areas) in percentage over time and show that the granularity of the community structure increases during financial stress periods. From the graph, it can be observed a high degree of granularity in the network structure from late-2007 to mid-2009 and from mid-2011 to late-2012 in the correspondence of the most acute phases of the Global financial crisis and the European sovereign debt crisis, respectively. This emphasizes once again that during the financial crises there has been a disintegration of the financial network in different groups of institutions with distinct connectivity patterns in the spread of contagion. Finally, we apply the new connectivity measures presented in Section 2.1

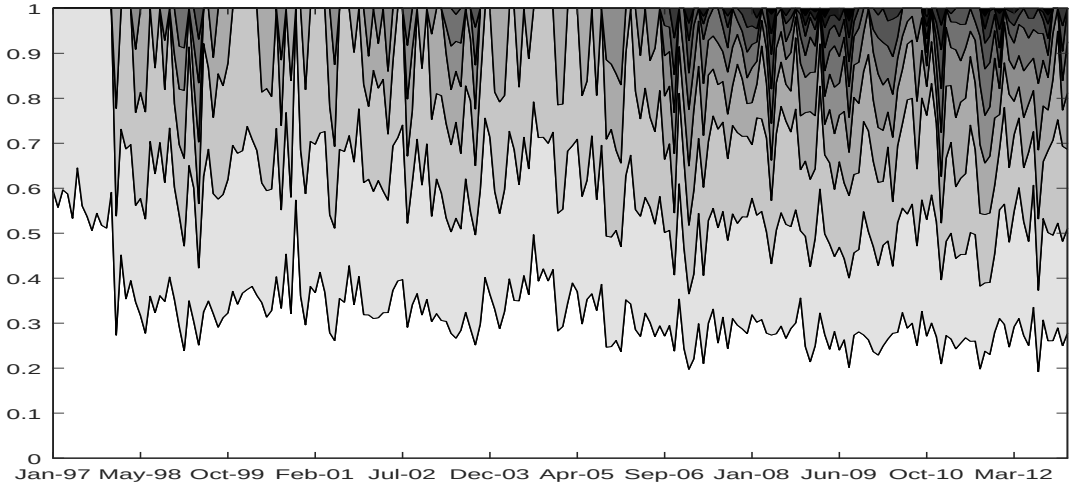

Figure 4: Size of the European financial communities (shaded areas) in percentage during 1996-2013. Each community has a different gray level.

on the European network. Figure 5 reports intra, inter communities and total network density measures where empirical correlations are equal to $\hat{\rho}_{intra,total}(0.50)$, $\hat{\rho}_{inter,total}(0.97)$ and $\hat{\rho}_{intra,inter}(0.30)$.

The total network density (f) is driven by the inter-community connectivity (f^{INTER}) with a residual role played by the intra-community one (f^{INTRA}). This suggests a disassortative structure of the network where the edges existing between the groups and thus, the community bridges, may play a relevant role in the spread of contagion in the financial system.

As a further confirmation, we report in Figure 6 the relative weight of the intra community (dashed line) and the inter-community (solid line) density which shows that except in the very beginning of the sample, the first is higher in all the considered period.

[8] As robustness checks, we include in Appendix C the estimation of the optimal block numbers with different window lengths.

Given that the European financial network exhibits a robust interdependent community structure, the identification of the SIFIs should not be reduced in terms of total connectedness but should instead be investigated by discriminating among intra and inter-community connectedness.[9]

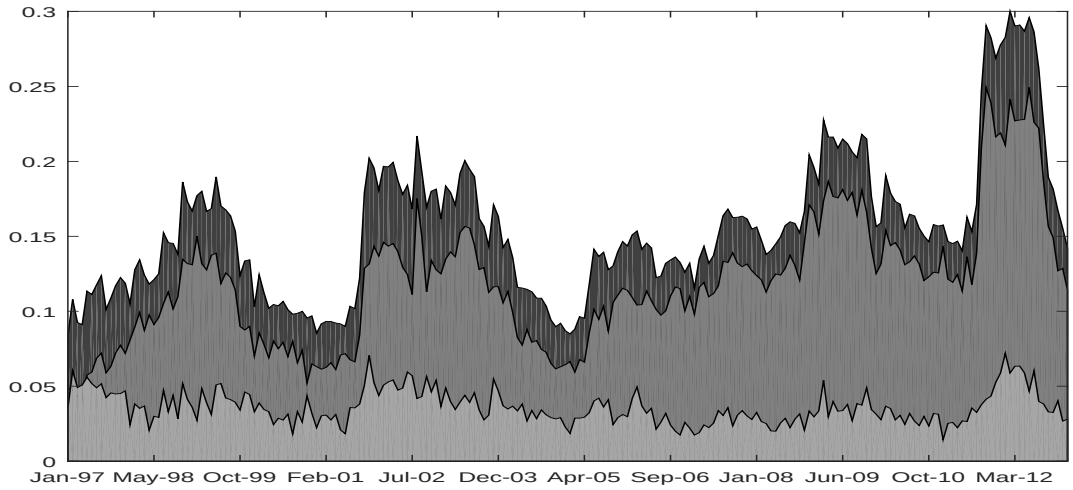

Figure 5: Density measures of the European network for intra community density (light grey), inter community density (grey) and total network density (dark grey) during 1996-2013.

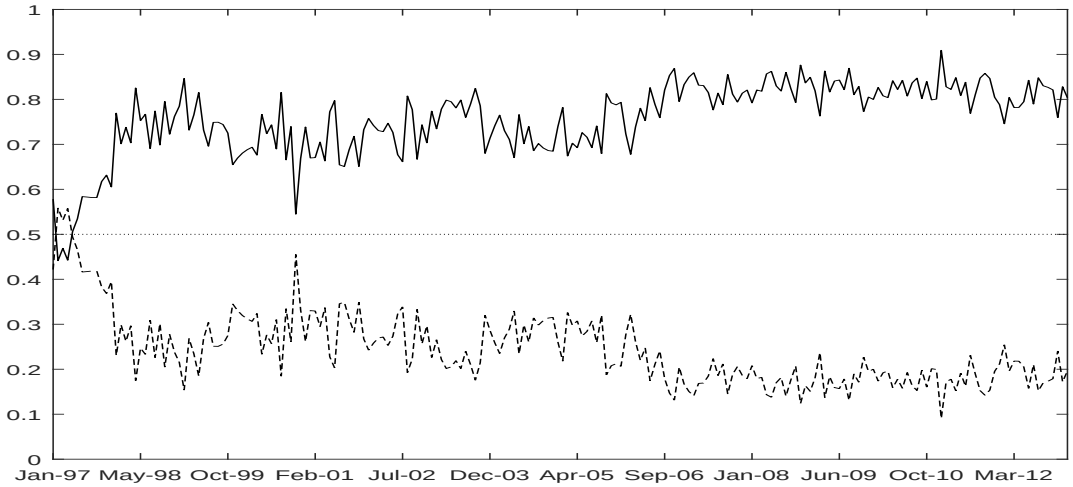

Figure 6: Relative weights of intra community (dashed line) and inter community (solid line) on the total network density during the period 1996-2013.

3.3 The Global Financial Crisis and the European Sovereign Debt Crisis

In the following section, we analyze the European financial network and its community structure during the Global financial crisis and the European sovereign debt crisis. Having a directed

[9] For sake of space, we report connectivity measures such as community intra and inter, in and out degrees in the Appendix D.

financial network, we can distinguish a community as a shock transmitter or receiver through the out inter-community degrees and in inter-community degrees, respectively. We attribute the systemically importance to a community by considering its role in the spread of contagion in the network, that is, the higher out inter-community degrees net of the in inter-community degrees with concerning the other communities.

The Global financial crisis

We select from the inferred European dynamic network the adjacency matrix on November 2008 which corresponds to the 155^{th} window. The aim is to analyze the European financial network during the Global financial crisis originated from the subprime mortgage market in the United States occurred from 2007 to 2008. Figure 7 includes the network with the community structures (10 communities). Panel (a) shows the directed network graph where edges are concave and clockwise directed while Panel (b) shows the adjacency matrix according to the community membership. The network is composed by 365 financial institutions: 62 Banks (red nodes), 39 Insurances (blue nodes), 84 Real Estate companies (green nodes) and 180 financial services institutions (black nodes) according to the ICB classification. The majority of the financial institutions are traded in the United Kingdom (186), Italy (50), Germany (37) and France (30). Table 1 reports the partitioned density according to the inter and intra linkages which shows

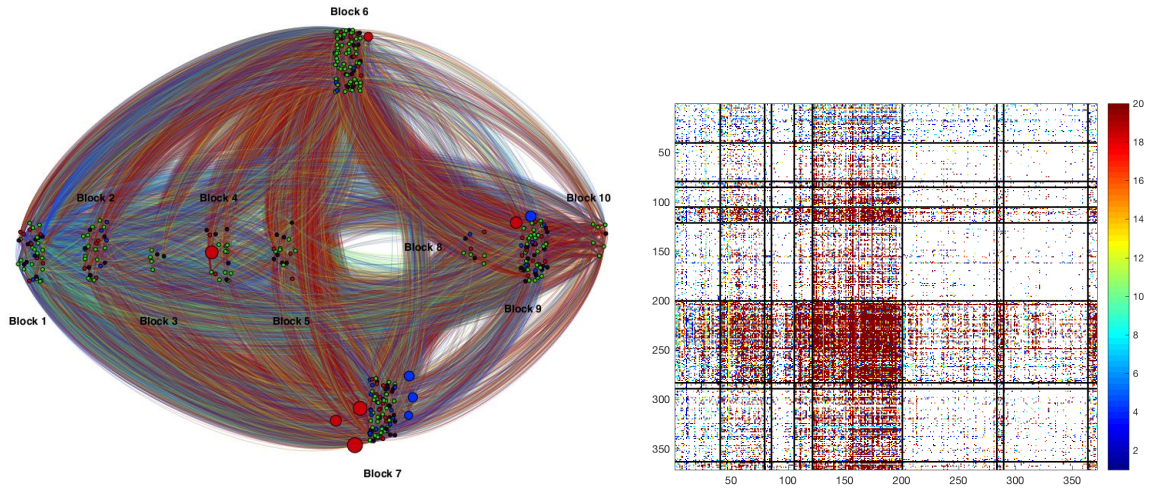

(a) Causality Network. (b) Adjacency matrix.

Figure 7: The European financial network (155^{th} window) during the global financial crisis. Edges color is reported according to the edges weight (see the colormap) while nodes color is reported according to the ICB: banks (red), insurances (blue), financial services (green) and real estate (black). Panel (a): Network diagrams. Edges are concave and clockwise directed where the size of nodes is reported according to the market value for the top 10 largest financial institution. Panel (b): Adjacency Matrix. Causality is meant from row i to column j.

that the total density of the network is 20.44%. According to community connectivity measures, Block 7 represents the systemically important financial community (SIFC) since it exhibits the highest net out-inter community density (7.91%), $f^{net,INTRA}$. It can be observed that the network exhibits a two core structure where one core (SIFC) spreads shocks almost exclusively to another one (Block 6) and hence, the inter-linkages among two communities represent ideally a bipartite network.

As reported in Table 3, Block 7 is composed by insurances (53.85% of the market), banks (29.03%), Real Estate (26.19%) and Financial Services (16.11%). It is worth noting that this block includes 6 out 10 (3 banks and 3 insurances) of the largest financial institution in terms of market value Figure 7(a) and represents the largest community in terms of total market value as reported in Table 2.[10] This is particularly interesting since networks here are inferred using only market returns for each financial institution and not other information such as market value is not considered in the process. On the other hand, Block 6 is the community that largely receives shocks from Block 7 (4.63%) and for the residual part by Block 9 (1.62%) as reported in Table 1.

Table 3 reports the European financial institutions according to the community memberships at the sub-sector level where the percentages describe the proportion of institutions of each community in a given sector. The SIFC contains the majority of the insurances in the market (53.85%) including nonlife insurances (33.33%) and life insurances (20.51%). The critical difference between life and nonlife insurances relies on the different time horizon of their products. Life insurances have longer-term policies in their business model and hence, they are longer-term investors. Generally, among other factors (i.e., a high leverage), investment performance represents a significant determinant for both the type of insurances (i.e., common exposure to sovereign and corporate bond risk).[11] Finally, the receiver block (Block 6) contains the largest group of institutions that are in the Financial services sector (35%) with a majority of equity investment instruments (26.11%) which includes corporate closed-ended investment entities such as investment trusts and venture capital trusts. The residual part includes Financial Services (8.89%).

The European sovereign debt crisis

The global financial crisis is considered the trigger for the European sovereign debt crisis occurred at the end of 2009 which brought a change in the asset prices and grew prospectively in the

[10] The weight of the 10 largest financial institutions are shown in Figure 7 using a different size of the vertex which depends on their market value.

[11] See Gründl et al. (2017) for a discussion about portfolio investment strategies for insurances.

	Block 1	Block 2	Block 3	Block 4	Block 5	Block 6	Block 7	Block 8	Block 9	Block 10	$f^{-,INTER}$	$f^{-net,INTER}$
Block 1	0.08%	0.11%	0.01%	0.03%	0.08%	0.81%	0.10%	0.03%	0.05%	0.04%	1.25%	0.05%
Block 2	0.03%	0.05%	0.01%	0.01%	0.03%	0.42%	0.04%	0.02%	0.01%	0.02%	0.60%	-1.14%
Block 3	0.01%	0.02%	0.00%	0.00%	0.01%	0.20%	0.00%	0.01%	0.00%	0.01%	0.26%	-0.07%
Block 4	0.02%	0.05%	0.01%	0.01%	0.03%	0.44%	0.03%	0.01%	0.02%	0.03%	0.64%	0.08%
Block 5	0.09%	0.11%	0.02%	0.03%	0.06%	0.64%	0.15%	0.03%	0.08%	0.04%	1.18%	0.11%
(receiver) Block 6	0.15%	0.23%	0.02%	0.03%	0.13%	1.71%	0.18%	0.05%	0.07%	0.08%	0.93%	-8.32%
(spreader) Block 7	0.70%	0.92%	0.21%	0.37%	0.60%	4.63%	1.31%	0.31%	0.66%	0.33%	8.71%	7.91%
Block 8	0.01%	0.03%	0.00%	0.00%	0.02%	0.18%	0.02%	0.01%	0.01%	0.01%	0.27%	-0.27%
Block 9	0.15%	0.21%	0.04%	0.06%	0.13%	1.62%	0.18%	0.07%	0.09%	0.09%	2.54%	1.59%
Block 10	0.05%	0.07%	0.01%	0.02%	0.04%	0.33%	0.11%	0.02%	0.05%	0.02%	0.70%	0.06%
$f^{+,INTER}$	1.20%	1.74%	0.32%	0.56%	1.07%	9.25%	0.81%	0.54%	0.95%	0.64%	20.44%	f

Table 1: Partitioned network density f, according to the community structure during the Global financial crisis. The diagonal elements reports the intra-density of each community (f^{INTRA}) and the off-diagonal elements the in (out) inter-density (f^{INTER}) according to the i_{th}-row (column) to j_{th}-column (row). Last row (second to last column) reports in (out) inter density, $f^{+,INTER}$ ($f^{-,INTER}$). The last column report the out inter community density net of in inter community density $f^{-net,INTER}$ and $f = f^{INTRA} + f^{INTER} = 3.34\% + 17.76\% = 20.44\%$. The density within each community: Block 1 (37.15%), Block 2 (57.09%), Block 3 (42.50%), Block 4 (47%), Block 5 (59.29%), Block 6 (73.97%), Block 7 (69.76%), Block 8 (59.06%), Block 9 (54.95%) and Block 10 (84.06%).

	Block 1	Block 2	Block 3	Block 4	Block 5	Block 6	Block 7	Block 8	Block 9	Block 10
Market Value	11.43	10.99	7.59	10.94	8.95	10.89	12.89	8.54	11.88	6.68

Table 2: The total market value in logarithmic form for each community during the Global financial crisis.

	Block 1	Block 2	Block 3	Block 4	Block 5	Block 6	Block 7	Block 8	Block 9	Block 10	Total
Banks	**12.90%**	**6.45%**		**4.84%**	**4.84%**	**17.74%**	**29.03%**	**3.23%**	**20.97%**		**100.00%**
Insurances	**5.13%**	**10.26%**				**10.26%**	**53.85%**	**2.56%**	**17.95%**		**100.00%**
Nonlife insurances	*5.13%*	*5.13%*				*7.69%*	*33.33%*		*17.95%*		69.23%
Full Line Insurance	5.13%	5.13%				2.56%	10.26%		7.69%		30.77%
Insurance Brokers						2.56%	2.56%		2.56%		7.69%
Property & Casualty Insurance						2.56%	10.26%		7.69%		20.51%
Reinsurance							10.26%				10.26%
Life insurances		*5.13%*				*2.56%*	*20.51%*	*2.56%*			30.77%
Real Estate	**13.10%**	**7.14%**	**2.38%**	**5.95%**	**8.33%**	**14.29%**	**26.19%**	**2.38%**	**19.05%**	**1.19%**	**100.00%**
Real Estate Investment & Services	*8.33%*	*4.76%*		*3.57%*	*3.57%*	*9.52%*	*16.67%*	*2.38%*	*10.71%*	*1.19%*	60.71%
Real Estate Holding & Development	8.33%	4.76%		3.57%	3.57%	9.52%	14.29%	2.38%	9.52%	1.19%	57.14%
Real Estate Services							2.38%		1.19%		3.57%
Real Estate Investment Trusts	*4.76%*	*2.38%*	*2.38%*	*2.38%*	*4.76%*	*4.76%*	*9.52%*		*8.33%*		39.29%
Industrial & Office REITs			1.19%	2.38%	3.57%	4.76%	4.76%		7.14%		23.81%
Retail REITs	2.38%	2.38%	1.19%				3.57%		1.19%		10.71%
Residential REITs					1.19%						1.19%
Diversified REITs											
Specialty REITs	2.38%						1.19%				3.57%
Mortgage REITs											
Hotel & Lodging REITs											
Financial Services	**10.56%**	**7.22%**	**2.22%**	**5.56%**	**3.33%**	**35.00%**	**16.11%**	**2.22%**	**14.44%**	**3.33%**	**100.00%**
Financial Services	*6.11%*	*3.89%*		*2.78%*		*8.89%*	*11.11%*		*8.33%*	*1.11%*	42.22%
Asset Managers	1.11%	0.56%				1.11%	3.33%		2.22%		8.33%
Consumer Finance		2.22%				1.11%					3.33%
Specialty Finance	4.44%			2.22%		5.00%	3.89%		2.78%	1.11%	19.44%
Investment Services	0.56%	0.56%		0.56%		1.67%	3.89%		2.78%		10.00%
Mortgage Finance		0.56%									0.56%
Equity Investment Instruments	*4.44%*	*3.33%*	*2.22%*	*2.78%*	*3.33%*	*26.11%*	*5.00%*	*2.22%*	*6.67%*	*2.22%*	58.33%
Nonequity Investment Instruments											
Relative size	**10.96%**	**7.40%**	**1.64%**	**4.93%**	**4.38%**	**24.66%**	**24.66%**	**2.47%**	**16.99%**	**1.92%**	**100.00%**

Table 3: European financial institutions according to the community and sector (sub-sector) membership during the Global financial crisis. The percentages describe the proportion of institutions of each community on a given sector (sub-sector) and are reported in columns 2-5. Last row reports the proportions of each community with respect to the total number of institutions in the market.

Eurozone. Lane (2012) provides an exhaustive analysis of pre-crisis risk factors discussing the relationship among the global financial crisis and the sovereign debt crisis.

In this regard, we select the adjacency matrix on April 2012 which corresponds to the 199^{th} window of the dynamic network. Figure 8 includes the community structures (eight communities). Panel (a) shows the directed network graph where edges are concave and clockwise directed while Panel (b) shows the adjacency matrix according to the community membership. The network is composed by 359 financial institutions: 58 Banks (red nodes), 33 Insurances (blue nodes), 82 Real Estate companies (green nodes) and 186 financial services institutions (black nodes). The majority of the financial institutions are traded in the United Kingdom (173), Germany (58), Italy (44) and France (34). As shown in Table 4, the total density of the

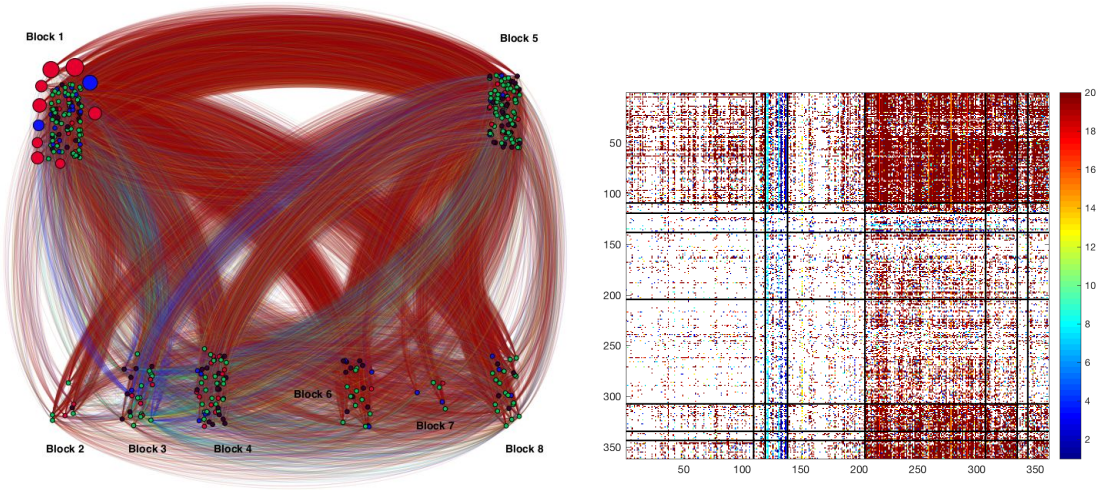

(a) Causality Network.

(b) Adjacency matrix.

Figure 8: The European financial network (199^{th} window) during the European sovereign debt crisis. Edges color is reported according to the edges weight (see the colormap) while nodes color is reported according to the ICB: banks (red), insurances (blue), financial services (green) and real estate (black). Panel (a): Network diagrams. Edges are concave and clockwise directed where the size of nodes is reported according to the market value for the top 10 largest financial institutions. Panel (b): Adjacency Matrix. Causality is meant from row i to column j.

network is 29.11% where Block 1 represents the SIFC since it exhibits the highest net out-inter community density (10.71%), $f^{net,INTRA}$. Even in this case, the European financial network exhibits a two cores structure where the SIFC (Block 1) spreads shocks mostly to another core (Block 5). The SIFC represents the largest community in terms of market value as shown in Table 5 and as during the global financial crisis, includes the majority of the insurances in the market (51.52%) with both nonlife (27.27%) and life insurances (24.24%). The block is composed by Insurances (51.52% of the total market), Banks (39.66%), Financial Services (30.65%) and

Real Estate (19.51%) as reported in Table 6. It is worth noting that the SIFC includes all the top ten financial institutions in terms of market value (8 banks and 2 insurances). Vice versa, Block 5 is the community that largely receives shocks from Block 1 (7.15%) and for a residual part mostly by Block 8 (1.50%), Block 6 (1.27%) and Block 4 (1.22%) as reported in Table 4. This block contains the largest group of institutions that are in the Financial services sector (34.41%) and the Real Estate sector (34.15%) with almost equal weights at their sub-sector level. Finally, Table 6 reports the European financial institutions according to the community memberships at the sub-sector level where the percentages describe the proportion of institutions of each community on a given sector. Once again, it highlights that the insurance industry played a prominent role in the spread of systemic risks also during the European sovereign debt crisis.

4 Financial Bridges and Policy Implications

In this Section, we compare the standard and the presented community connectivity measures in predicting financial losses. Moreover, we assess their impact on the European financial network in terms of contagion. The aim is to determine if the inclusion of the community structure (i.e., financial bridges) in the European financial network provides a better measurement of financial connectedness.

4.1 Early Warning Indicators

As seen in Section 3.2, the density of the network is driven mainly by the inter-community connections which highlight the role of financial bridges in the spread of contagion. Following Billio et al. (2012) and Acharya et al. (2017), we perform an out-of-sample analysis of the presented community measures with respect to the usual network measures and compare their predictive ability concerning future losses. In this regard, we define the variable *MaxLoss*, the maximum loss incurred by a single institution within the next two years and use total out and inter- (intra-) community out degrees as predictors in the linear model:

$$MaxLoss_i = c + \beta X_i + \varepsilon_i, \quad \varepsilon_i \overset{iid}{\sim} (0, \sigma^2),$$

where $i = 1, \ldots, n$ and $X_i = \{d_i^-, d_i^{-,INTER}, d_i^{-,INTRA}\}$ is expressed in relative value to make the coefficients comparable. We perform the cross-sectional regressions sequentially from 2000 to 2012 and report in Figure 9 the adjusted R-squared, the magnitude and p-value of each coefficient.

	Block 1	Block 2	Block 3	Block 4	Block 5	Block 6	Block 7	Block 8	$f^{-,INTER}$	$f^{-net,INTER}$
(spreader) Block 1	2.77%	0.27%	0.58%	1.00%	7.15%	1.69%	0.20%	1.37%	12.26%	10.71%
Block 2	0.08%	0.01%	0.03%	0.04%	0.36%	0.07%	0.01%	0.06%	0.64%	0.19%
Block 3	0.15%	0.02%	0.04%	0.08%	0.46%	0.09%	0.01%	0.08%	0.88%	-0.34%
Block 4	0.23%	0.02%	0.11%	0.19%	1.22%	0.23%	0.02%	0.14%	1.97%	0.11%
(receiver) Block 5	0.33%	0.05%	0.25%	0.35%	2.79%	0.50%	0.04%	0.27%	1.78%	-10.44%
Block 6	0.31%	0.04%	0.11%	0.15%	1.27%	0.27%	0.03%	0.19%	2.11%	-0.86%
Block 7	0.06%	0.00%	0.02%	0.03%	0.26%	0.05%	0.01%	0.03%	0.47%	0.11%
Block 8	0.39%	0.05%	0.12%	0.20%	1.50%	0.34%	0.04%	0.26%	2.64%	0.51%
$f^{+,INTER}$	1.55%	0.45%	1.22%	1.86%	12.22%	2.97%	0.36%	2.13%	29.11%	f

Table 4: Partitioned network density f, according to the community structure during the European sovereign crisis. The diagonal elements reports the intra-density of each community (f^{INTRA}) and the off-diagonal elements the in (out) inter-density (f^{INTER}) according to the i_{th}-row (column) to j_{th}-column (row). Last row (second to last column) reports in (out) inter density, $f^{+,INTER}$ ($f^{-,INTER}$). The last column report the out inter community density net of the in inter community density $f^{-net,INTER}$ and $f = f^{INTRA} + f^{INTER} = 6.34\% + 22.76\% = 29.11\%$. The density within each community: Block 1 (87.71%), Block 2 (92.86%), Block 3 (39.06%), Block 4 (73.73%), Block 5 (83.70%), Block 6 (92.49%), Block 7 (88.50%) and Block 8 (90.20%).

	Block 1	Block 2	Block 3	Block 4	Block 5	Block 6	Block 7	Block 8
Market Value	13.47	8.39	9.17	11.10	11.00	9.94	9.09	10.57

Table 5: The total market value in logarithmic form for each community during the European sovereign debt crisis.

	Block 1	Block 2	Block 3	Block 4	Block 5	Block 6	Block 7	Block 8	Total
Banks	**39.66%**	**3.45%**	**8.62%**	**24.14%**	**15.52%**	**1.72%**	**1.72%**	**5.17%**	**100.00%**
Insurances	**51.52%**		**3.03%**	**18.18%**	**12.12%**	**9.09%**	**6.06%**		**100.00%**
Nonlife insurances	*27.27%*			*18.18%*	*9.09%*	*6.06%*	*6.06%*	*6.06%*	72.73%
Full Line Insurance	12.12%			9.09%	3.03%	3.03%		3.03%	30.30%
Insurance Brokers	6.06%			3.03%					9.09%
Property & Casualty Insurance	3.03%			6.06%	6.06%	3.03%	6.06%		24.24%
Reinsurance	6.06%							3.03%	9.09%
Life insurances	*24.24%*		*3.03%*		*3.03%*	*3.03%*		*3.03%*	36.36%
Real Estate	**19.51%**	**1.22%**	**8.54%**	**18.29%**	**34.15%**	**13.41%**		**4.88%**	**100.00%**
Real Estate Investment & Services	*8.54%*		*6.10%*	*14.63%*	*17.07%*	*9.76%*		*1.22%*	57.32%
Real Estate Holding & Development	7.32%		4.88%	10.98%	17.07%	9.76%		1.22%	51.22%
Real Estate Services	1.22%		1.22%	3.66%					6.10%
Real Estate Investment Trusts	*10.98%*	*1.22%*	*2.44%*	*3.66%*	*17.07%*	*3.66%*		*3.66%*	42.68%
Industrial & Office REITs	4.88%	1.22%	1.22%	2.44%	8.54%	2.44%		2.44%	23.17%
Retail REITs	6.10%			1.22%	2.44%	1.22%		1.22%	12.20%
Residential REITs					1.22%				1.22%
Diversified REITs			1.22%		1.22%				2.44%
Specialty REITs					2.44%				2.44%
Mortgage REITs									
Hotel & Lodging REITs					1.22%				1.22%
Financial Services	**30.65%**	**2.15%**	**5.91%**	**10.75%**	**34.41%**	**5.38%**	**1.61%**	**9.14%**	**100.00%**
Financial Services	*10.75%*		*3.76%*	*8.60%*	*14.52%*	*2.69%*	*1.08%*	*1.08%*	42.47%
Asset Managers	2.15%		1.08%		4.30%		0.54%	1.08%	9.14%
Consumer Finance	0.54%				1.08%	0.54%			2.15%
Specialty Finance	5.38%		2.15%	5.38%	5.38%	2.15%	0.54%		20.97%
Investment Services	2.69%			2.69%	3.23%				8.60%
Mortgage Finance					0.54%				0.54%
Equity Investment Instruments	*19.89%*	*2.15%*	*2.69%*	*2.69%*	*19.89%*	*2.69%*	*0.54%*	*8.06%*	58.60%
Nonequity Investment Instruments									
Relative Size	**31.48%**	**1.95%**	**6.69%**	**15.32%**	**29.25%**	**6.96%**	**1.67%**	**6.69%**	**100.00%**

Table 6: European financial institutions according to the community and sector (sub-sector) membership during the European Sovereign debt crisis. The percentages describe the proportion of institutions of each community on a given sector (sub-sector) and are reported in columns 2-5. Last row reports the proportions of each community with respect to the total number of institutions in the market.

The out-inter community degrees (dashed line) provide the best fitting over the total out degrees (solid line) in more than the 93% of the total cases while the out-intra community degrees (dashed line) provide the lowest performance in every period. At 5% significance level, the p-value analysis shows a significance of 79% for the total out degrees (solid line), 85% for out-inter community degrees (dashed line) and 13% for the out-intra community degrees (dotted line). Clearly, this implies that the total out degrees represents improved significant determinants of the *MaxLoss* variable. For the total out degrees and the out-inter community degrees, the coefficient is negative in more than 99% of the total significant cases which further indicates that the nodes with the highest out degrees incur into lower losses with respect to the other nodes. The order of magnitude is always greater for the inter-community out degrees (dashed line) with respect to the total out degrees (solid line) pointing out that losses for the firsts are lower. These findings highlight the primary role of the community inter-linkages in spreading shocks and represent a better early warning indicator for financial losses in the system with respect to the (standard) total out degrees. As a further comparison, we include in Appendix E the regression with the eigenvector centrality measure which confirms the previous results.[12]

4.2 Node impact on Contagion

Policy authorities act through prevention and mitigation measures to maintain financial stability. When a systemic risk arises in the network, policy interventions should immunize the node-spreaders in order to avoid the financial contagion. As stated in Salathé and Jones (2010), the presence of a community structure significantly affects the dynamic of the disease, and in such cases, immunization interventions should focus on community bridges instead of the nodes which are highly connected to the whole network.

We perform a simple immunization exercise by switching off recursively the node with: i) the highest total out degrees (global immunization); ii) the highest eigenvector centrality (centrality immunization) and iii) the highest community inter out degrees (community immunization). We make use of the average shortest path length (ASPL) as the evaluation criteria to compare the impact of a node immunization on financial contagion.

The ASPL measures the average number of steps along the shortest paths for all possible pairs of network nodes,

$$ASPL_t = \big[n_t(n_t-1)\big]^{-1} \sum_{i,j}^{n_t} d(i,j), \tag{10}$$

[12] We also perform the analysis for the total in and inter- (intra-) connections. Results for financial bridges confirm what described for the out-connections and are available upon request to the authors.

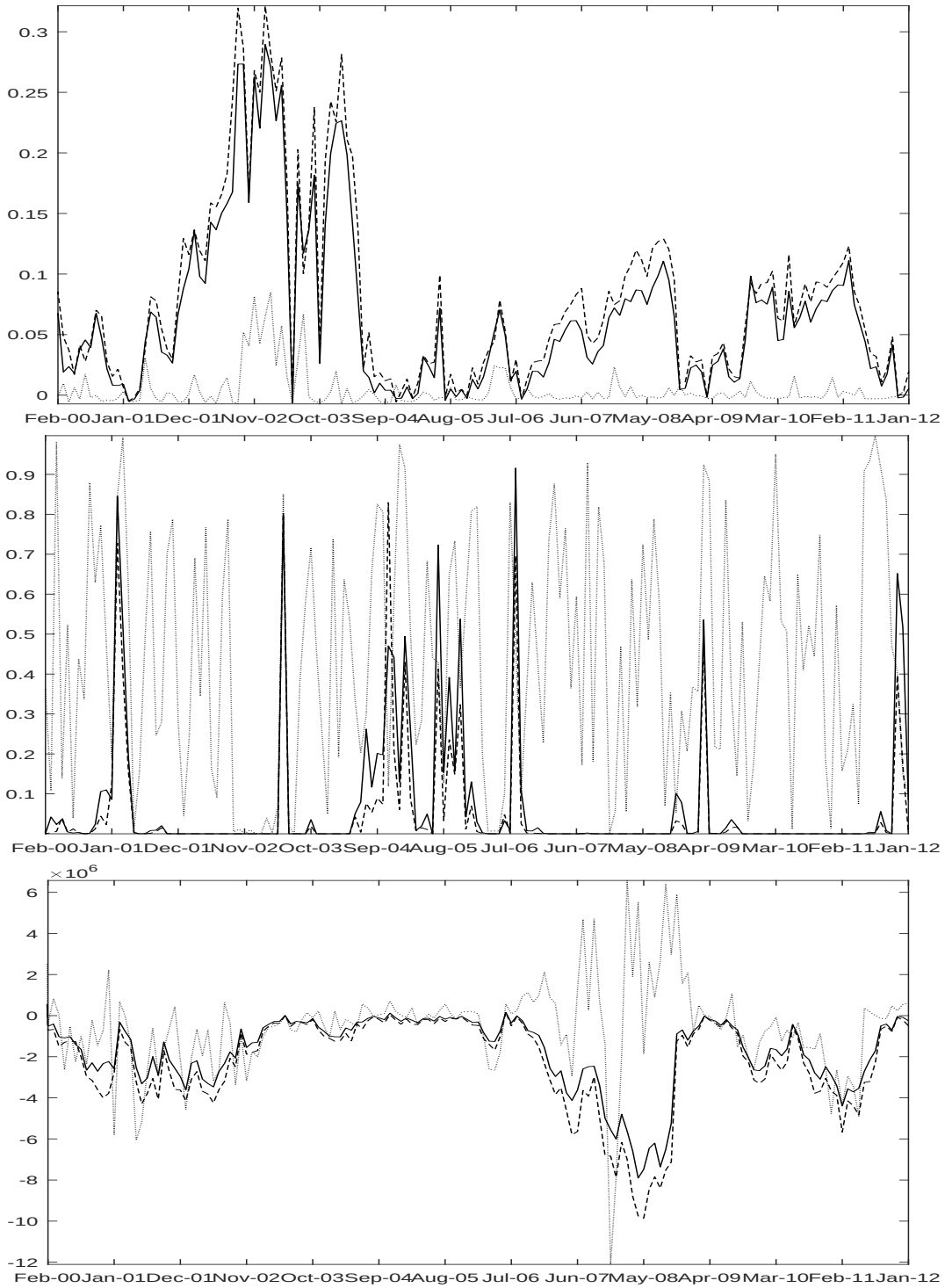

Figure 9: Adjusted R–squared (top), coefficient p-value (mid) and coefficient magnitude (bottom) for the cross-sectional regressions where the dependent variable is the maximum loss incurred by a single institution within the next two years and the independent variable is alternatively the total out degrees (solid line), the out-inter community degrees (dashed line) and the out-intra community degrees (dotted line).

where n_t is the number of nodes in the network and $d(i, j)$ is the shortest path from node i to node j. The ASPL indicates the number of financial institutions that an institution has to affect on average in order to transmit a shock to another institution which is not directly connected with it.

With the immunization of a node, the mitigation of (financial) contagion succeeds if there is an increase on the ASPL in the network, that is, the number of steps on average increases and thus, network becomes more robust to shock propagation. Conversely, if the ASPL decreases, the intervention is not only useless but harmful since the network is more exposed to financial instability.

As an example of policy intervention, we perform the analysis for the three type of immunizations on the financial network during the European sovereign debt crisis (199^{th} window of the estimated dynamic networks). Figure 10 shows the resulting ASPL after removing up to 15 nodes in the network. The community immunization (dashed red line) performs overall better than the global immunization (solid black line) and the centrality immunization (dotted black line). After the removal of the first node, the marginal contribution of each node is higher concerning the other considered cases. Therefore, the immunization of the financial network with a community structure is more effective through treatments on community bridges than usual connectedness measures. In fact, total inter out degrees converges towards an ASPL value of 4.25 after the immunization of 15 nodes while the total out degrees and the eigenvector centrality reach a value of 4.19 and 4.20, respectively. As a robustness check, we compute ASPL on all the period (210 networks) after removing 25 nodes. The ASPL is higher for the community inter out degrees more than the 67% of the cases.

5 Conclusion

This paper analyses financial contagion allowing for community structures in the network. Accordingly, we show that the total connectedness measures can be decomposed in inter- and intra-community connectedness providing a better description of the network connectivity patterns. We provide evidence of an increasing number of financial communities during periods of instability and identify financial bridges as responsible for spreading contagion through the network. Our findings show that during the recent crises, the European financial network exhibits a two cores structure with the presence of a community which contains the majority of insurances in the market and acts mainly as a shock spreader to a second community. The

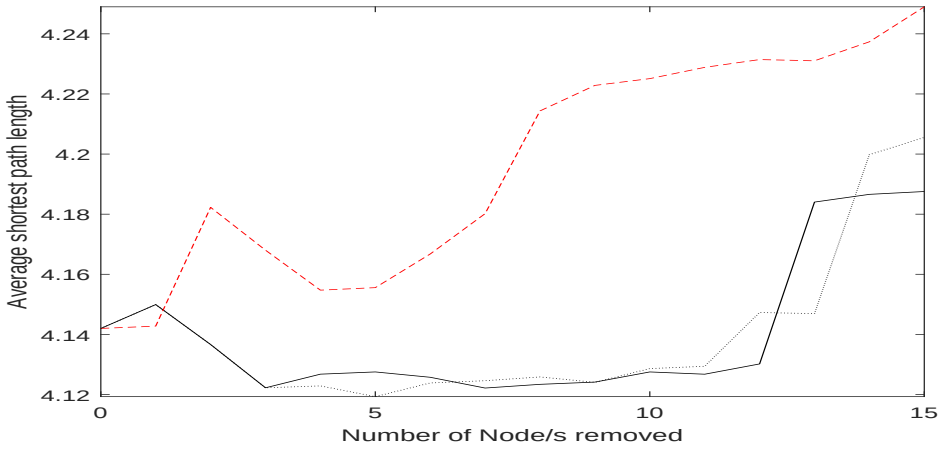

Figure 10: Average shortest path length (ASPL) after removing sequentially the node(s) with the highest total out degrees (solid black line), the highest eigenvector centrality (dotted black line) and the highest inter-community out degrees (dashed red line).

results reveal that the largest inter-community degrees generated by financial bridges represent a better early warning indicator for financial losses with respect to the total network degree. Finally, we perform an immunization exercise showing that monitoring and adopting treatments for financial bridges would represent a more effective mitigation policy than the one based on total degree connectedness. This would help regulators' and policymakers to respond promptly to abrupt changes of an evolving financial system.

References

Acemoglu, D., Ozdaglar, A., and Tahbaz-Salehi, A. (2015). Systemic Risk and Stability in Financial Networks. *American Economic Review*, 105(2):564–608.

Acharya, V. V., Biggs, J., Le, H., Richardson, M., and Ryan, S. (2011). *Systemic Risk and the Regulation of Insurance Companies*, chapter 9, pages 241–301. Wiley-Blackwell.

Acharya, V. V., Pedersen, L. H., Philippon, T., and Richardson, M. (2017). Measuring Systemic Risk. *The Review of Financial Studies*, 30(1):2–47.

Acharya, V. V., Philippon, T., and Richardson, M. (2016). *Measuring Systemic Risk for Insurance Companies*, chapter 5, pages 100–136. Oxford University Press.

Ahelegbey, D. F., Billio, M., and Casarin, R. (2016a). Bayesian Graphical Models for Structural Vector Autoregressive Processes. *Journal of Applied Econometrics*, 31(2):357–386.

Ahelegbey, D. F., Billio, M., and Casarin, R. (2016b). Sparse Graphical Vector Autoregression: A Bayesian Approach. *Annals of Economics and Statistics*, 123/124:333–361.

Aicher, C., Jacobs, A. Z., and Clauset, A. (2014). Learning latent block structure in weighted networks. *Journal of Complex Networks*, 3(2):221–248.

Allen, F. and Carletti, E. (2013). What Is Systemic Risk? *Journal of Money, Credit and Banking*, 45:121–127.

Allen, L., Bali, T. G., and Tang, Y. (2012). Does Systemic Risk in the Financial Sector Predict Future Economic Downturns? *The Review of Financial Studies*, 25(10):3000–3036.

Baranoff, E. G. and Sager, T. W. (2009). The Impact of Mortgage-Backed Securities on Capital Requirements of Life Insurers in the Financial Crisis of 2007–2008. *The Geneva Papers on Risk and Insurance-Issues and Practice*, 34(1):100–118.

Bargigli, L. and Gallegati, M. (2013). Finding communities in credit networks. *Economics*, 7(17):1.

Bates, J. M. and Granger, C. W. (1969). The Combination of Forecasts. *Journal of the Operational Research Society*, 20(4):451–468.

Billio, M., Getmansky, M., Lo, A. W., and Pelizzon, L. (2012). Econometric measures of connectedness and systemic risk in the finance and insurance sectors. *Journal of Financial Economics*, 104(3):535–559.

Blei, D. M., Kucukelbir, A., and McAuliffe, J. D. (2017). Variational inference: A review for statisticians. *Journal of the American Statistical Association*, 112(518):859–877.

Brewer, E., Carson, J. M., Elyasiani, E., Mansur, I., and Scott, W. L. (2007). Interest Rate Risk and Equity Values of Life Insurance Companies: A GARCH–M Model. *Journal of Risk and Insurance*, 74(2):401–423.

Brownlees, C. and Engle, R. F. (2017). SRISK: A Conditional Capital Shortfall Measure of Systemic Risk. *Review of Financial Studies*, 30(1):48–79.

Caccioli, F., Shrestha, M., Moore, C., and Farmer, J. D. (2014). Stability analysis of financial contagion due to overlapping portfolios. *Journal of Banking & Finance*, 46:233–245.

Cifuentes, R., Ferrucci, G., and Shin, H. S. (2005). Liquidity Risk and Contagion. *Journal of the European Economic Association*, 3(2-3):556–566.

de Souza, S. R. S., Silva, T. C., Tabak, B. M., and Guerra, S. M. (2016). Evaluating systemic risk using bank default probabilities in financial networks. *Journal of Economic Dynamics and Control*, 66:54–75.

Diebold, F. X. and Yılmaz, K. (2014). On the network topology of variance decompositions: Measuring the connectedness of financial firms. *Journal of Econometrics*, 182(1):119–134.

Diebold, F. X. and Yilmaz, K. (2015). *Financial and Macroeconomic Connectedness: A Network Approach to Measurement and Monitoring*. Oxford University Press.

Ellul, A., Jotikasthira, C., and Lundblad, C. T. (2011). Regulatory pressure and fire sales in the corporate bond market. *Journal of Financial Economics*, 101(3):596–620.

Financial Stability Board (2009). Guidance to Assess the Systemic Importance of Financial Institutions, Markets and Instruments: Initial Considerations.

Fortunato, S. (2010). Community detection in graphs. *Physics reports*, 486(3-5):75–174.

Franklin Allen, A. B. (2009). *Networks in Finance*, chapter 21, pages 367–382. Pearson Prentice Hall.

Freixas, X., Parigi, B. M., and Rochet, J.-C. (2000). Systemic Risk, Interbank relations, and Liquidity Provision by the Central Bank. *Journal of Money, Credit and Banking*, 32(3):611–638.

Giglio, S., Kelly, B., and Pruitt, S. (2016). Systemic risk and the macroeconomy: An empirical evaluation. *Journal of Financial Economics*, 119(3):457–471.

Gründl, H., Gal, J., et al. (2017). The evolution of insurer portfolio investment strategies for long-term investing. *OECD Journal: Financial Market Trends*, 2016(2):1–55.

Hałaj, G. and Kok, C. (2013). Assessing interbank contagion using simulated networks. *Computational Management Science*, 10(2-3):157–186.

Haldane, A. G. (2013). Rethinking the financial network. In *Fragile stabilität–stabile fragilität*, pages 243–278. Springer.

Haldane, A. G. and May, R. M. (2011). Systemic risk in banking ecosystems. *Nature*, 469(7330):351.

Hautsch, N., Schaumburg, J., and Schienle, M. (2015). Financial Network Systemic Risk Contributions. *Review of Finance*, 19(2):685–738.

Holland, P. W., Laskey, K. B., and Leinhardt, S. (1983). Stochastic blockmodels: First steps. *Social Networks*, 5(2):109–137.

Hollo, D., Kremer, M., and Lo Duca, M. (2012). CISS - A Composite Indicator of Systemic Stress in the Financial System. *ECB Working Paper Series, 1426*.

Huang, A., Wand, M. P., et al. (2013). Simple Marginally Noninformative Prior Distributions for Covariance Matrices. *Bayesian Analysis*, 8(2):439–452.

Jackson, M. (2010). *Social and Economic Networks*. Princeton University Press.

Karrer, B. and Newman, M. E. (2011). Stochastic blockmodels and community structure in networks. *Physical Review E*, 83(1):016107.

Lane, P. R. (2012). The European Sovereign Debt Crisis. *The Journal of Economic Perspectives*, 26(3):49–67.

Leicht, E. A. and Newman, M. E. J. (2008). Community Structure in Directed Networks. *Phys. Rev. Lett.*, 100:118703.

McGrory, C. A. and Titterington, D. (2007). Variational approximations in Bayesian model selection for finite mixture distributions. *Computational Statistics & Data Analysis*, 51(11):5352–5367.

Newman, M. (2018). *Networks*. Oxford University Press.

Penny, W., Kiebel, S., and Friston, K. (2003). Variational bayesian inference for fMRI time series. *NeuroImage*, 19(3):727–741.

Pham, T. H., Ormerod, J. T., and Wand, M. P. (2013). Mean field variational Bayesian inference for nonparametric regression with measurement error. *Computational Statistics & Data Analysis*, 68:375–387.

Puliga, M., Flori, A., Pappalardo, G., Chessa, A., and Pammolli, F. (2016). The Accounting Network: How Financial Institutions React to Systemic Crisis. *PLOS One*, 11(10).

Salathé, M. and Jones, J. H. (2010). Dynamics and Control of Diseases in Networks with Community Structure. *PLoS Computational Biology*, 6(4):e1000736.

Scott, H. S. (2016). *Connectedness and Contagion: Protecting the Financial System from Panics.* MIT Press.

Shleifer, A. and Vishny, R. (2011). Fire Sales in Finance and Macroeconomics. *Journal of Economic Perspectives*, 25(1):29–48.

Shumway, T. (1997). The delisting bias in CRSP data. *The Journal of Finance*, 52(1):327–340.

Teschendorff, A. E., Wang, Y., Barbosa-Morais, N. L., Brenton, J. D., and Caldas, C. (2005). A variational Bayesian mixture modelling framework for cluster analysis of gene-expression data. *Bioinformatics*, 21:3025–3033.

Thomson, J. B. (2010). On Systemically Important Financial Institutions and Progressive Systemic Mitigation. *DePaul Business & Commercial Law Journal*, 8:135–419.

Titterington, D. M. (2004). Bayesian Methods for Neural Networks and Related Models. *Statistical Science*, 19(1):128–139.

Tobias, A. and Brunnermeier, M. K. (2016). CoVar. *The American Economic Review*, 106(7):1705.

Wand, M. P., Ormerod, J. T., Padoan, S. A., Frühwirth, R., et al. (2011). Mean field variational Bayes for elaborate distributions. *Bayesian Analysis*, 6(4):847–900.

A Modelling Communities

In this Section, we introduce time-varying stochastic block models for community detection and present a inference approach.

A.1 Stochastic Block Models

We extend to a dynamic context the SBM and weighted SBM models given in Aicher et al. (2014).

Let $G_t = (V_t, E_t)$, $t = 1, \ldots, T$ be a time sequence of networks, with vertex set V_t and edge set $E_t \subset V_t \times V_t$, and let A_t be the $n_t \times n_t$ adjacency matrix of the network G_t, which contains binary values representing edge existence, i.e. $A_{ij,t} \in \{0, 1\}$ with $A_{ij,t} = 1$ if $(i, j) \in E_t$ and $A_{ij,t} = 0$ otherwise, $i, j = 1, \ldots, n_t$ where n_t is the cardinality of V_t.

We assume $t_0 < t_1 < t_2 < \ldots < t_M < t_{M+1}$, with $t_0 = 1$ and $t_{M+1} = T$, is a sequence of change points. The network parameters and the label vector are constant within a sub-period, but change over sub-periods $[t_{m-1}, t_m]$, and the edge distribution for the network at time t is

$$g(A_t|\mathbf{z}, \boldsymbol{\theta}) = \begin{cases} f(A_t|\mathbf{z}_1, \boldsymbol{\theta}_1) & 0 < t \leq t_1 \\ f(A_t|\mathbf{z}_2, \boldsymbol{\theta}_2) & t_1 < t \leq t_2 \\ \ldots & \ldots \\ f(A_t|\mathbf{z}_M, \boldsymbol{\theta}_M) & t_M < t \leq T \end{cases}$$

where $f(A|\mathbf{z}_M, \boldsymbol{\theta}_M)$ is an edge probability model discussed in the following paragraph, $\boldsymbol{\theta} = (\boldsymbol{\theta}_1, \ldots, \boldsymbol{\theta}_M)$ is the collection of period-specific parameters and $\mathbf{z} = (\mathbf{z}_1, \ldots, \mathbf{z}_M)$ is the collection of period-specific latent variable vectors.

Here, we present the models for the edge probabilities and drop for the sake of simplicity the time subscript t. In the basic SBM, there are K latent groups of nodes and the probability p_{ij} of an edge between nodes i and j, i.e., $\Pr((i, j) \in E)$ depends on the groups the two nodes belong, that is

$$p_{ij} = \theta_{z_i z_j}^{A_{ij}} (1 - \theta_{z_i z_j})^{1 - A_{ij}} \tag{11}$$

$i, j = 1, \ldots, n$, where $z_i \in \{1, \ldots, K\}$ indicates which group the node i belongs to. The existence probability of an edge A_{ij} is given by the parameter θ_{z_i, z_j} that depends only on the membership of nodes i and j. Note that, in Equation 11, the A_{ij}s are conditionally independent given z_i, $i = 1, \ldots, n$ and θ_{kl}, $k, l = 1, \ldots, K$. The probability that $z_i = k$ is equal to γ_{ik}, with

$k = 1, \ldots, K$. We assume γ_{ik} equals to γ_k. The number of latent groups, K, is a free parameter that must be chosen before the model and it controls the model's complexity.

Let $\mathbf{z} = (z_1, \ldots, z_n)$ be the $(n \times 1)$ vector that contains the labels of the nodes. Then, vector z represents the partition of the nodes into K blocks, and each pair of groups (k, l) represents a bundle of edge between the groups. The parameter $\boldsymbol{\theta}$ in Equation 11 represents a $(K \times K)$ matrix, the affinity matrix, with (l, k)-element the edge probability parameter θ_{lk}. From Equation 11, the joint probability distribution of the edge existence for a given network G can be written as follows:

$$f(A|\mathbf{z}, \boldsymbol{\theta}) = \prod_{(i,j)\in E} \exp\left(A_{ij} \cdot \log\left(\frac{\theta_{z_i z_j}}{1 - \theta_{z_i z_j}}\right) + \log(1 - \theta_{z_i z_j})\right),$$

which belongs to the exponential family, since it has the following kernel

$$f(A|\mathbf{z}, \boldsymbol{\theta}) \propto \exp\left(\sum_{(i,j)\in E} \boldsymbol{\tau}(A_{ij}) \cdot \boldsymbol{\eta}(\theta_{z_i z_j})\right), \tag{12}$$

where $\boldsymbol{\tau}(x) = (x, 1)'$ is the vector-valued function of sufficient statistics of a Bernoulli distribution and $\boldsymbol{\eta}(\theta) = (\log(\theta/(1-\theta)), \log(1-\theta))$ is a vector-valued function of natural parameters. This is a basic and classical SBM for unweighted networks since, as they are defined, the functions $\boldsymbol{\tau}$ and $\boldsymbol{\eta}$ produce binary edge values.

The latent allocation variables z_i follow a discrete uniform distribution

$$z_i \overset{i.i.d.}{\sim} \mathcal{U}_{\{1,\ldots,K\}}, \quad i = 1, \ldots, n, \tag{13}$$

which implies $\gamma_k = 1/K$. For the edge probability parameter θ, we assume a conjugate non-informative prior, that is

$$\theta_{kk'} \overset{i.i.d.}{\sim} \mathcal{U}_{[0,1]}, \quad k, k' = 1, \ldots, K. \tag{14}$$

With a different and appropriate choice of the functions $\boldsymbol{\tau}$ and $\boldsymbol{\eta}$, a WSBM can be established by weights that are drawn from an exponential family distribution over the domain of $\boldsymbol{\tau}$. In this case, each $\boldsymbol{\theta}_{z_i z_j} = (\mu_{z_i z_j}, \sigma_{z_i, z_j})'$ denotes the parameters governing the weight distribution of the edge bundle $(z_i z_j)$ and the edge weight probability is

$$f(A|\mathbf{z}, \boldsymbol{\theta}) \propto \exp\left(\sum_{(i,j)\in W} \boldsymbol{\tau}(A_{ij}) \cdot \boldsymbol{\eta}(\boldsymbol{\theta}_{z_i z_j})\right), \tag{15}$$

where the pair of functions $(\boldsymbol{\tau}, \boldsymbol{\eta})$ for the real valued edge weights is needed.

Networks with real valued edge weights can be modelled by an exponential family distribution. We consider a normal distribution with parameters μ and σ^2 and define with $\boldsymbol{\tau}(x) = \left(x, x^2, 1\right)$ the vector of sufficient statistics and with $\boldsymbol{\eta}(\boldsymbol{\theta}) = (\mu/\sigma^2, -1/(2\sigma^2), -\mu^2/(2\sigma^2))$ the natural parameter vector. The latent allocation variables z_i follow a discrete uniform distribution, that is

$$z_i \overset{i.i.d.}{\sim} \mathcal{U}_{\{1,\ldots,K\}}, i = 1, \ldots, n. \tag{16}$$

For the parameter $\boldsymbol{\theta}$, we assume a conjugate non-informative prior, that is

$$\sigma^2_{kk'} \overset{i.i.d.}{\sim} \frac{1}{\sigma^2_{kk'}} \mathbb{I}_{\mathbb{R}^+}(\sigma^2_{kk'}), \quad \mu_{kk'} \overset{i.i.d.}{\sim} \mathbb{I}_{\mathbb{R}}(\mu_{kk'}), \quad k, k' = 1, \ldots, K. \tag{17}$$

The SBM and pure WSBM models produce complete graphs which can be an undesirable features in large dimension networks. In order to model sparse networks by SBM and WSBM, Aicher et al. (2014) assumes $A_{ij} = 0$ as a directed edge from node i to j is existed with zero weight, thus parse networks can be modelled with two types of information, edge existence and edge weight values, in together by a simple tuning parameter, that is:

$$f(A|\mathbf{z}, \boldsymbol{\theta}) \propto \exp\left(\alpha \sum_{(i,j)\in E} \boldsymbol{\tau}_e(A_{ij}) \cdot \boldsymbol{\eta}_e(\theta^{(e)}_{z_i z_j}) + (1-\alpha) \sum_{(i,j)\in W} \boldsymbol{\tau}_w(A_{ij}) \cdot \boldsymbol{\eta}_e(\theta^{(w)}_{z_i z_j})\right) \tag{18}$$

where the pair $(\boldsymbol{\tau}_e, \boldsymbol{\eta}_e)$ denotes the family of edge existence distribution and the pair $(\boldsymbol{\tau}_w, \boldsymbol{\eta}_w)$ denotes the family of edge-weight distribution, $\alpha \in [0, 1]$ is a simple tuning parameter that combines their contributions in the edge probability. E is the set of observed interactions (including non-edges) and W is the set of weighted edges with $W \subset E$.

If $\alpha = 1$ (Equation 18), then the model reduces to SBM in Equation 11, and if $\alpha = 0$, the model ignores edge existence information and we refer to such model as the pure WSBM (pWSBM). When $0 < \alpha < 1$, the edge distribution combines both information set, and if $\alpha = 0.5$ the model is called balanced WSBM (Aicher et al., 2014).

For the SBM part, in Equation 18, we assume $\boldsymbol{\tau}_e(x) = (x, 1)'$ and $\boldsymbol{\eta}_e(\theta) = (\log(\theta/(1-\theta)), \log(1-\theta))$. For the pure WSBM part, in Equation 18, we assume $\boldsymbol{\tau}_w(x) = \left(x, x^2, 1\right)$ and $\boldsymbol{\eta}_w(\boldsymbol{\theta}) = (\mu/\sigma^2, -1/(2\sigma^2), -\mu^2/(2\sigma^2))$ the natural parameter vector. Finally we define with $\boldsymbol{\theta} = \{P, \boldsymbol{\mu}, \boldsymbol{\sigma}\}$ the parameter vector with $P = (\theta_{ij})_{ij}$, $\boldsymbol{\mu} = (\mu_1, \ldots, \mu_K)$ and $\boldsymbol{\sigma} = (\sigma_1, \ldots, \sigma_K)$.

A.2 Bayesian Inference for Stochastic Block Models

Let $A_{m-1:m}$ be the collection of matrices from time $t_{m-1}+1$ to time t_m, i.e. $A_{m-1:m} = \{A_{t_{m-1}+1}, \ldots, A_{t_m}\}$. In our change-point models, we assume in each sub-sample the allocation and parameter vectors, $\mathbf{z}_m$ and $\boldsymbol{\theta}_m$, respectively, are constant, thus the likelihood function of our SBM is

$$\mathcal{L}(A_{1:M}|\mathbf{z}_{1:M}, \boldsymbol{\theta}_{1:M}) \propto \prod_{m=1}^{M} \exp\left(\sum_{ij} \boldsymbol{\tau}_e\left(\bar{A}_{ij,m}\right) \cdot \boldsymbol{\eta}_e(\theta_{k,z_{im}z_{jm}})\right) \tag{19}$$

where $\bar{A}_{ij,m}$ is the (i,j)-the element of the matrix

$$\bar{A}_m = \sum_{t=t_{m-1}+1}^{t_m} A_t \tag{20}$$

and $\boldsymbol{\tau}_e(x) = (x, d)$ is the vector-valued function of sufficient statistics and $\boldsymbol{\eta}_e(\theta) = (\log(\theta/(1-\theta)), \log(1-\theta))$ is the vector-valued function of natural parameters. See subsection A.3 for a proof.

Since for the WSBM each edge bundle $(z_{im}z_{jm})$ is now parametrized by a mean and variance, $\theta_{z_{im}z_{jm}} = (\mu_{z_{im}z_{jm}}, \sigma^2_{z_{im},z_{jm}})$, the likelihood of the pure WSBM can be written as:

$$\mathcal{L}(A_{1:M}|\mathbf{z}_{1:M}, \boldsymbol{\theta}_{1:M}) \propto \prod_{m=1}^{M} \exp\left(\sum_{ij} \boldsymbol{\tau}_w\left(\bar{A}_{ij,m}\right) \cdot \boldsymbol{\eta}_w(\theta_{k,z_{im}z_{jm}})\right) \tag{21}$$

where $\boldsymbol{\tau}_w(x) = \left(x, x^2, d\right)$ and $\boldsymbol{\eta}_w(\boldsymbol{\theta}) = (\mu/\sigma^2, -1/(2\sigma^2), -\mu^2/(2\sigma^2))$. See subsection A.3 for a proof.

The likelihood of the general WSBM can be obtained by combining Equation 19 and Equation 21 with combining parameter $\alpha \in [0,1]$, that is.

$$\begin{aligned}\mathcal{L}(A_{1:M}|\mathbf{z}_{1:M}, \boldsymbol{\theta}_{1:M}) &= \exp\left(\alpha\left(\sum_{m=1}^{M}\sum_{ij} \boldsymbol{\tau}_e\left(\bar{A}_{ij,m}\right) \cdot \boldsymbol{\eta}_e(\theta_{m,z_{im}z_{jm}})\right)\right. \\ &+ \left.(1-\alpha)\left(\sum_{m=1}^{M}\sum_{ij} \boldsymbol{\tau}_w\left(\bar{A}_{ij,m}\right) \cdot \boldsymbol{\eta}_w(\theta_{m,z_{im}z_{jm}})\right)\right)\end{aligned} \tag{22}$$

where the pair $(\boldsymbol{\tau}_e, \boldsymbol{\eta}_e)$ denotes the family of edge existence distribution and the pair $(\boldsymbol{\tau}_w, \boldsymbol{\eta}_w)$ denotes the family of edge-weight distribution. E is the set of observed interactions (including non-edges) and W is the set of weighted edges with $W \subset E$ and α is a tuning parameter which

combines the contributions of edge existence and edge weight information in the likelihood function. See subsection A.3 for a proof.

The posterior distribution of model in Equation 18 is intractable, but can be approximated by using several methods. Markov Chain Monte Carlo (MCMC) can be an efficient approach with a high computational cost. Thus, in this paper, we follow Aicher et al. (2014) and apply variational Bayes methods to circumvent this issue. Variational Bayes approximation has been successfully applied in many fields such as neural science (e.g. Penny et al., 2003), and biostatistics (e.g. Teschendorff et al., 2005) where high dimensional models or large datasets make MCMC methods are not feasible. Variational Bayes approximation is now popular also in statistics (e.g., see McGrory and Titterington (2007), Titterington (2004), Wand et al. (2011), Pham et al. (2013),Huang et al. (2013)). See also Blei et al. (2017) for an up-to-date review. The parameters K, number of blocks, and α, tuning parameter, are crucial in our application. Selection of optimal K and α can be achieved by applying Bayes factor. The selection of the tuning parameter, α, is left and we considered in the application three different values of α: 0 (pure WSBM), 0.5 (balanced WSBM) and 1 (basic SBM).

A.3 Proofs of the Results in Section A.2

i. Proof of the results in Eq. 19

For the observations in the sample period from $t_{m-1}+1$ to t_m the likelihood is

$$\begin{aligned}\mathcal{L}(A_{m:m+1}|\mathbf{z}_m,\boldsymbol{\theta}_k) &= \prod_{t=t_{m-1}+1}^{t_m}\prod_{(i,j)\in E_m}\theta_{z_{im}z_{jm}}^{A_{ij,t}}(1-\theta_{m,z_{im}z_{jm}})^{1-A_{ij,t}},\\ &= \prod_{i=1}^{n}\prod_{j=1}^{n}(\theta_{m,z_{im}z_{jm}})^{\sum_{t=t_{m-1}+1}^{t_m}A_{ij,t}}(1-\theta_{m,z_{im}z_{jm}})^{\sum_{t=t_{m-1}+1}^{t_m}(1-A_{ij,t})} \qquad (23)\end{aligned}$$

which can be written in exponential form as

$$\begin{aligned}\mathcal{L}(A_{m:m+1}|\mathbf{z}_m,\boldsymbol{\theta}_k) &= \prod_{i=1}^{n}\prod_{j=1}^{n}\exp\left(\sum_{t=t_{m-1}+1}^{t_m}A_{ij,t}\cdot\log\theta_{m,z_{im}z_{jm}}+\left(\sum_{t}^{n}(1-A_{ij,t})\right)\cdot\log(1-\theta_{m,z_{im}z_{jm}})\right)\\ &= \prod_{i=1}^{n}\prod_{j=1}^{n}\exp\left(\sum_{t=t_{m-1}+1}^{t_m}A_{ij,t}\cdot\log\left(\frac{\theta_{m,z_{im}z_{jm}}}{1-\theta_{m,z_{im}z_{jm}}}\right)+d\cdot\log(1-\theta_{m,z_{im}z_{jm}})\right)\end{aligned}$$

By using the exponential family representation of the density the above equation can be written

as

$$\mathcal{L}(A_{m:m+1}|\mathbf{z}_m, \boldsymbol{\theta}_k) \propto \exp\left(\sum_{i=1}^{n}\sum_{j=1}^{n}\sum_{t=t_{m-1}+1}^{t_m} \boldsymbol{\tau}_e^*\left(A_{ij,t}\right) \cdot \boldsymbol{\eta}_e(\theta_{m,z_{im}z_{jm}})\right) \tag{24}$$

$$\propto \exp\left(\sum_{i=1}^{n}\sum_{j=1}^{n} \boldsymbol{\tau}_e\left(\bar{A}_{ij,m}\right) \cdot \boldsymbol{\eta}_e(\theta_{m,z_{im}z_{jm}})\right) \tag{25}$$

with $\boldsymbol{\tau}_e^*(x) = (x, 1)$, $\boldsymbol{\tau}_e(x) = (x, d)$ and $\boldsymbol{\eta}_e(x) = (\log(x/(1-x)), \log(1-x))$.

Finally, the likelihood function of the change-point SBM is

$$\mathcal{L}(A_{1:M}|\mathbf{z}_{1:M}, \boldsymbol{\theta}_{1:M}) \propto \prod_{m=1}^{M} \mathcal{L}(A_{m:m+1}|\mathbf{z}_m, \boldsymbol{\theta}_m)$$

$$\propto \exp\left(\sum_{m=1}^{M}\sum_{i=1}^{n}\sum_{j=1}^{n} \boldsymbol{\tau}_e\left(\bar{A}_{ij,m}\right) \cdot \boldsymbol{\eta}_e(\theta_{m,z_{im}z_{jm}})\right) \tag{26}$$

□

ii. Proof of the results in Eq. 21

$$\mathcal{L}(A_{m:m+1}|\mathbf{z}_m, \boldsymbol{\theta}_k) = \prod_{t=t_{m-1}+1}^{t_m} \prod_{(i,j)\in W_m} \mathcal{N}\left(A_{ij,t}|\mu_{m,z_{im}z_{jm}}, \sigma^2_{m,z_{im}z_{jm}}\right)$$

$$= \prod_{i=1}^{n}\prod_{j=1}^{n} \exp\left(\sum_{t=t_{m-1}+1}^{t_m} A_{ij,t} \cdot \frac{\mu_{m,z_{im}z_{jm}}}{\sigma^2_{m,z_{im}z_{jm}}} - \sum_{t=t_{m-1}+1}^{t_m} A^2_{ij,t} \cdot \frac{1}{2\sigma^2_{m,z_{im}z_{jm}}} - d \cdot \frac{\mu^2_{m,z_{im}z_{jm}}}{2\sigma^2_{m,z_{im}z_{jm}}}\right)$$

$$\propto \exp\left(\sum_{ij} \boldsymbol{\tau}_w\left(\bar{A}_{ij}\right) \cdot \boldsymbol{\eta}_w(\boldsymbol{\theta}_{m,z_{im}z_{jm}})\right)$$

where $\boldsymbol{\tau}_w(x) = \left(x, x^2, d\right)$ and $\boldsymbol{\eta}_w(\boldsymbol{\theta}) = (\mu/\sigma^2, -1/(2\sigma^2), -\mu^2/(2\sigma^2))$. Finally, the likelihood function of the change-point pure WSBM is

$$\mathcal{L}(A_{1:M}|\mathbf{z}_{1:M}, \boldsymbol{\theta}_{1:M}) \propto \prod_{m=1}^{M} \mathcal{L}(A_{m:m+1}|\mathbf{z}_m, \boldsymbol{\theta}_m)$$

$$\propto \exp\left(\sum_{m=1}^{M}\sum_{i=1}^{n}\sum_{j=1}^{n} \boldsymbol{\tau}_w\left(\bar{A}_{ij}\right) \cdot \boldsymbol{\eta}_w(\boldsymbol{\theta}_{m,z_{im}z_{jm}})\right) \tag{27}$$

□

iii. Proof of the results in Eq. 22

Following the same line as in the proof of Eq. 19 and Eq. 21 we obtain

$$\mathcal{L}(A_{m:m+1}|\mathbf{z}_m, \boldsymbol{\theta}_k) \propto \exp\left(\sum_{ij} \boldsymbol{\tau}_e\left(\bar{A}_{ij,m}\right) \cdot \boldsymbol{\eta}_e(\theta_{m,z_{im}z_{jm}}) + \sum_{ij} \boldsymbol{\tau}_w\left(\bar{A}_{ij}\right) \cdot \boldsymbol{\eta}_w(\boldsymbol{\theta}_{m,z_{im}z_{jm}})\right)$$

the likelihood function of the change-point WSBM is

$$\begin{aligned}\mathcal{L}(A_{1:M}|\mathbf{z}_{1:M}, \boldsymbol{\theta}_{1:M}) &\propto \prod_{m=1}^{M} \mathcal{L}(A_{m:m+1}|\mathbf{z}_m, \boldsymbol{\theta}_m) \\ &\propto \exp\left(\sum_{m=1}^{M}\sum_{ij} \boldsymbol{\tau}_e\left(\bar{A}_{ij,m}\right) \cdot \boldsymbol{\eta}_e(\theta_{m,z_{im}z_{jm}}) + \sum_{m=1}^{M}\sum_{ij} \boldsymbol{\tau}_w\left(\bar{A}_{ij}\right) \cdot \boldsymbol{\eta}_w(\boldsymbol{\theta}_{m,z_{im}z_{jm}})\right) \quad (28)\end{aligned}$$

□

B Optimal Number of Block and Model Selection

In this section, we consider three settings of the WSBM: i) the SBM with $\alpha = 1$; ii) the balanced WSBM with $\alpha = 0.5$ and iii) the pure WSBM with $\alpha = 0$. First, we select the optimal number of blocks for each window obtained with the three considered models and then compare the community structure across the models. Second, we perform the model selection according to their predictive ability through the tuning parameter α, and we discuss the optimal block numbers as an indicator of systemic risk.

B.1 Optimal Number of Blocks

We select the optimal number of blocks through the marginal log-likelihoods approximated by the lower bound, $G(q)$, of each model and then, we compare them by varying the number of communities, K, from 1 to the number of total nodes in the network n. The optimal number

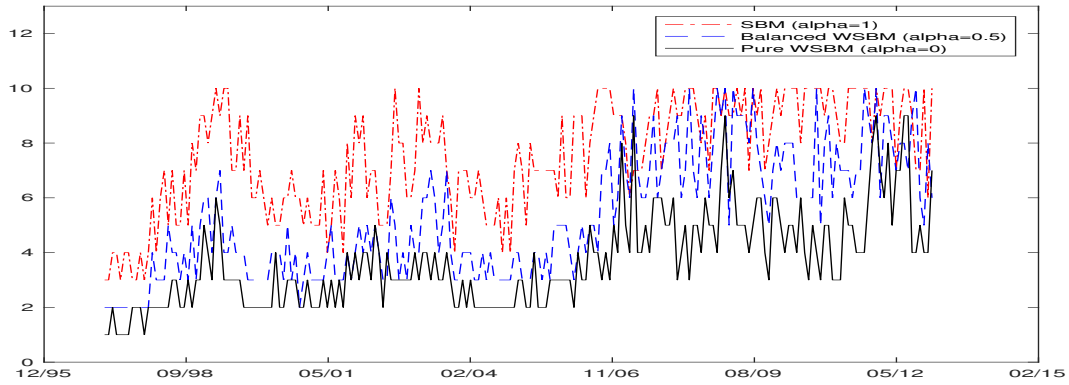

Figure 11: The optimal number of latent blocks, K, over time: black dash-dot line ($\alpha = 1$), red solid line and blue dashed line represent $\alpha = 0.5$ and $\alpha = 0$ respectively.

of latent blocks over time with three different values of tuning parameter α are reported in Figure 11. It is observable that the optimal number of blocks of all the three considered models increases during crisis periods reaching their highest levels. Clearly, the optimal block number depends on the specified model. Mostly, the values of the optimal block number with $\alpha = 1$ and $\alpha = 0$ act as an upper and lower bound for the model $\alpha = 0.5$, respectively. The optimal block number reaches its highest level (10) in 50 windows for the SBM ($\alpha = 1$) model while the balanced WSBM ($\alpha = 0.5$) reaches this level only in 13 windows. In the pure WSBM ($\alpha = 0$), the highest number of optimal block is 7. The series is reported in Table 7.

We proceed with the selection of the model by comparing the SBM ($\alpha = 1$), the balanced WSBM ($\alpha = 0.5$) and the pure WSBM ($\alpha = 0$), and then we discuss the selection of tuning parameter, α. We fix the number of blocks K equal to 4 in order to make a viable comparison

With $\alpha = 1$			With $\alpha = 0.5$			With $\alpha = 0$		
K	Windows	Percent	K	Windows	Percent	K	Windows	Percent
2	11	5.26%	2	15	7.18%	2	53	25.36%
3	7	3.35%	3	28	13.40%	3	60	28.71%
4	47	22.49%	4	51	24.40%	4	31	14.83%
5	37	17.70%	5	25	11.96%	5	22	10.53%
6	18	8.61%	6	22	10.53%	6	27	12.92%
7	3	1.44%	7	15	7.18%	7	10	4.78%
8	14	6.70%	8	22	10.53%	8	6	2.87%
9	22	10.53%	9	18	8.61%	9	0	0.00%
10	50	23.92%	10	13	6.22%	10	0	0.00%

Table 7: The optimal block numbers of the models, SBM ($\alpha = 1$), balanced WSBM ($\alpha = 0.5$) and pure WSBM ($\alpha = 0$).

and show the structural difference of the communities among considered models. The 18^{th} network is obtained from SBM ($\alpha = 1$), Balanced WSBM ($\alpha = 0.5$) and Pure WSBM ($\alpha = 0$) and reported in Figure 12. The standard deviation of edge weights for the WSBM is rather lower than the ones of SBM ($\alpha = 1$) since the model learns from both edge existence and edge weight information. In pure WSBM ($\alpha = 0$), the blocks are rather homogeneous in terms of in and out degree as in Figure 12(c)-(d))which is quite expected since pure WSBM ($\alpha = 0$) learns only from the edge weight information. Therefore, except for the pure WSBM, each block has different connectivity characteristics in SBM and balanced WSBM networks. On the other hand, each block has different edge weight level characteristics in pure WSBM (see Figure 12(c)-(d)).

B.2 Model Selection and α-Calibration

The selection of the tuning parameter (α) represents a crucial step in terms of modeling decision. The ideal choice should prefer the model which can exploit all the available information such as connectedness and edge weights information. Thus, we compare the performances of the models in terms of edge and edge weight prediction performances to show the ability of each model. The combined forecast method introduced in Bates and Granger (1969) is applied by giving equal weights to each of individual forecasts of SBM ($\alpha = 1$), WSBM ($\alpha = 0.5$) and pure WSBM ($\alpha = 0$). To show the contribution of each model's forecast performance out of the combined forecast for each window, the following calculation is done:

$$W_{it} = \frac{MSE_{it}^{-1}}{\sum_{i=1}^{3} MSE_{it}^{-1}}, \quad i = 1, 2, 3 \quad \text{and} \quad t = 1, 2, \ldots, 209 \tag{29}$$

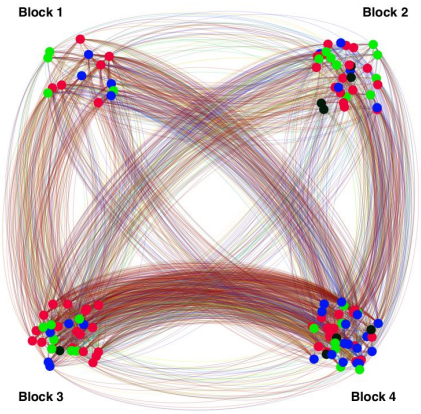

(a) SBM ($\alpha = 1$)

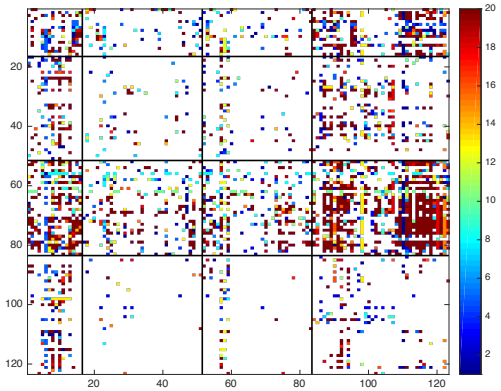

(b) SBM Adjacency Matrix

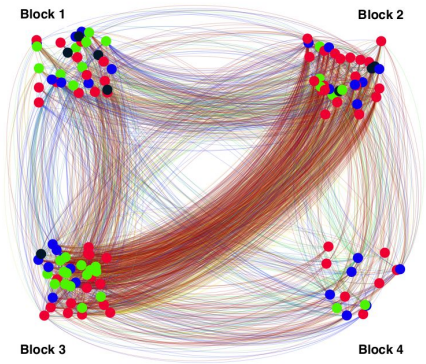

(c) Balanced WSBM ($\alpha = 0.5$)

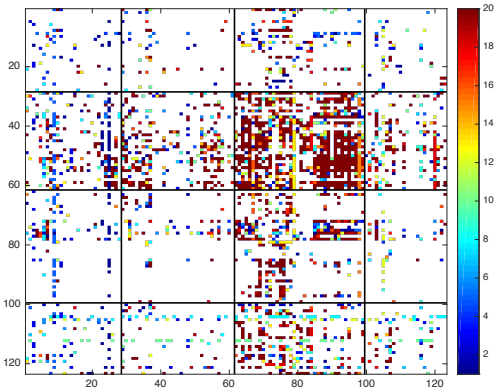

(d) Balanced WSBM Adjacency Matrix

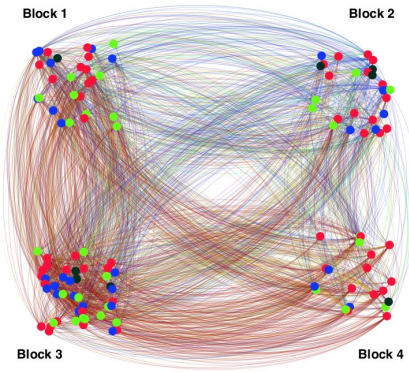

(e) Pure WSBM ($\alpha = 0$)

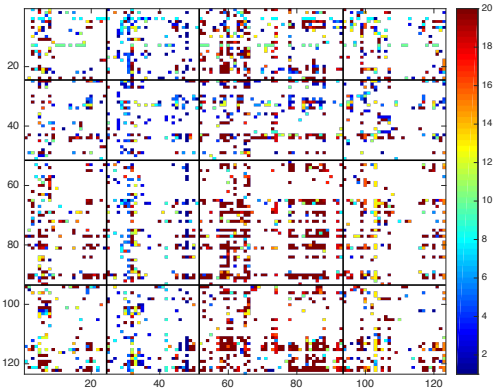

(f) Pure WSBM Adjacency Matrix

Figure 12: The European financial network (18^{th} window) on May 1998.
Edges color is reported according to the edges weight (see the colormap) while nodes color is reported according to the ICB: banks (red), insurances (blue), financial services (green) and real estate (black). Left Panels: Network diagrams. Edges are concave and clockwise directed where the size of nodes is reported according to the market value for the top 10 largest financial institution. Right Panels: Adjacency Matrix. Causality is meant from row i to column j.

where t represents the number of the window, t^{th} window, MSE indicates average mean square error, and i is the model type: $i = 1$ denotes SBM ($\alpha = 1$), $i = 2$ balanced WSBM ($\alpha = 0.5$) and $i = 3$ pure WSBM ($\alpha = 0$). W_{it} indicates the relative forecast performance of model i at the t^{th} window. Therefore, by Equation 29, $W_{it} > W_{-it}$ indicates the best forecast performance at window t is model.

The relative forecast performances of all the models are presented in Figure 13 by combined forecast method. The balanced WSBM ($\alpha = 0.5$) performs better on edge and edge weight prediction tasks (see Figure 13(a)). Besides, we analyze the features of the models in detail and report results on edge existence, and edge weights predictions separately in Figure 13(b)-(c).

As shown in Figure 13(b), the SBM and the balanced WSBM prove to be the most accurate models. As expected, the SBM show a better predictive ability in edge existence with respect to the balanced WSBM ($\alpha = 1$) given it only accounts for edge existence. Not surprisingly, the poorest model on edge prediction task is the pure WSBM ($\alpha = 0$) which considers only weight existence. On the edge weights prediction task, however, the pure WSBM ($\alpha = 0$) is the most accurate, often by a large margin and it is also expected well because it is modeled to learn only from edge weight information (see Figure 13(c)). The balanced WSBM ($\alpha = 0.5$) also performs quite accurate on the edge weight prediction task as nearly as the pure WSBM ($\alpha = 0$). The SBM ($\alpha = 1$), however, is the worst model on edge weight prediction task which is quite expected by construction.

In general, the SBM ($\alpha = 1$) is the best model for the performance of edge prediction but very poor on edge weight predictions. The pure WSBM performs accurate on weight prediction but it is very poor on edge prediction. However, the balanced WSBM is the only model which performs well on both tasks (see Figure 13). It performs as well as the SBM in edge prediction and substantially better than the SBM in edge weight prediction. In other words, the balanced WSBM is a more powerful model either than the SBM and pure WSBM in terms of prediction performances.

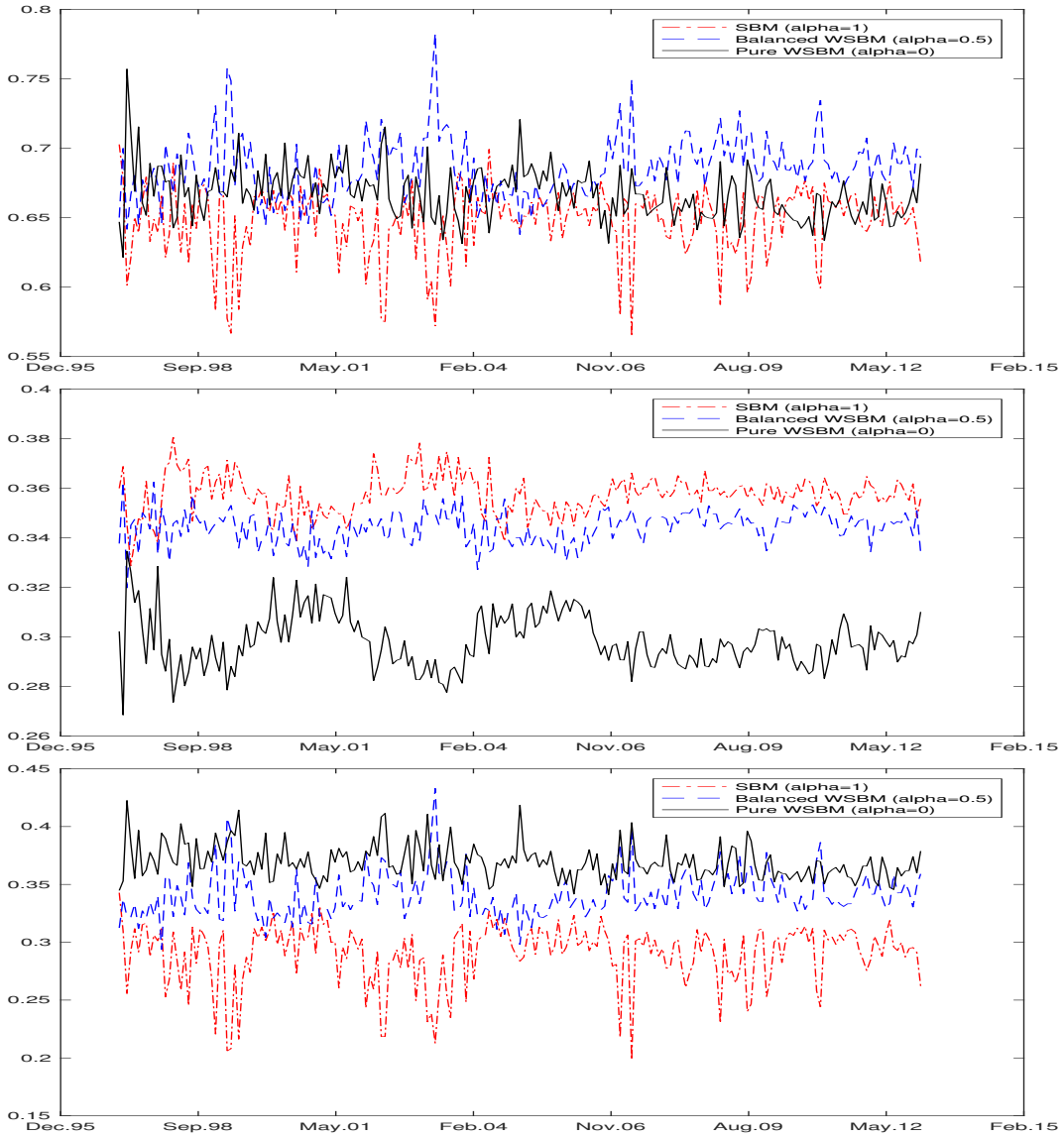

Figure 13: Edge existence and weight predictions performances of the models: a) Edge existence and edge weight prediction performances of the models (Top panel); b) Performances of the models only on edge existence predictions (Mid panel) and c) Performances of the models only on edge weight predictions (Bottom panel).

C Robustness Checks

As a robustness check, we estimate the optimal block numbers with different window lengths of 5, 10, 15, 20, 25 and 30 business days. As shown in Figure 14, the dynamic of the optimal number of K is not affected and remains stable with different window lengths.

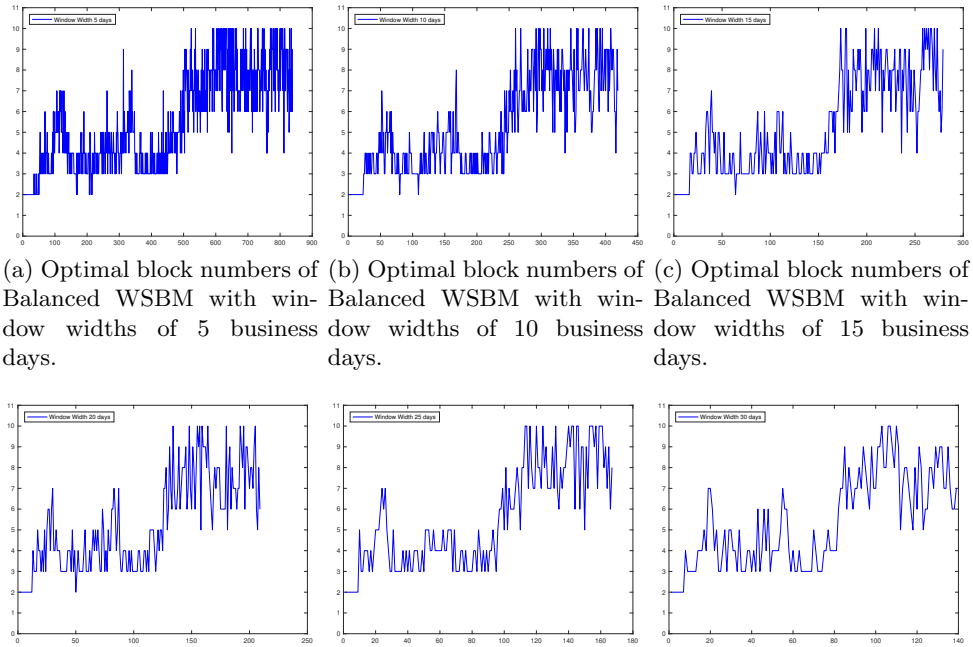

(a) Optimal block numbers of Balanced WSBM with window widths of 5 business days.

(b) Optimal block numbers of Balanced WSBM with window widths of 10 business days.

(c) Optimal block numbers of Balanced WSBM with window widths of 15 business days.

(d) Optimal block numbers of Balanced WSBM with window widths of 20 business days.

(e) Optimal block numbers of Balanced WSBM with window widths of 25 business days.

(f) Optimal block numbers of Balanced WSBM with window widths of 30 business days.

Figure 14: Robustness of the optimal number of blocks with different non-overlapping window widths

D Additional Connectivity Measures

In this section, we report in Figure 15 additional connectivity measures such as in(out), in(out)-inter and in(out)-intra degrees.

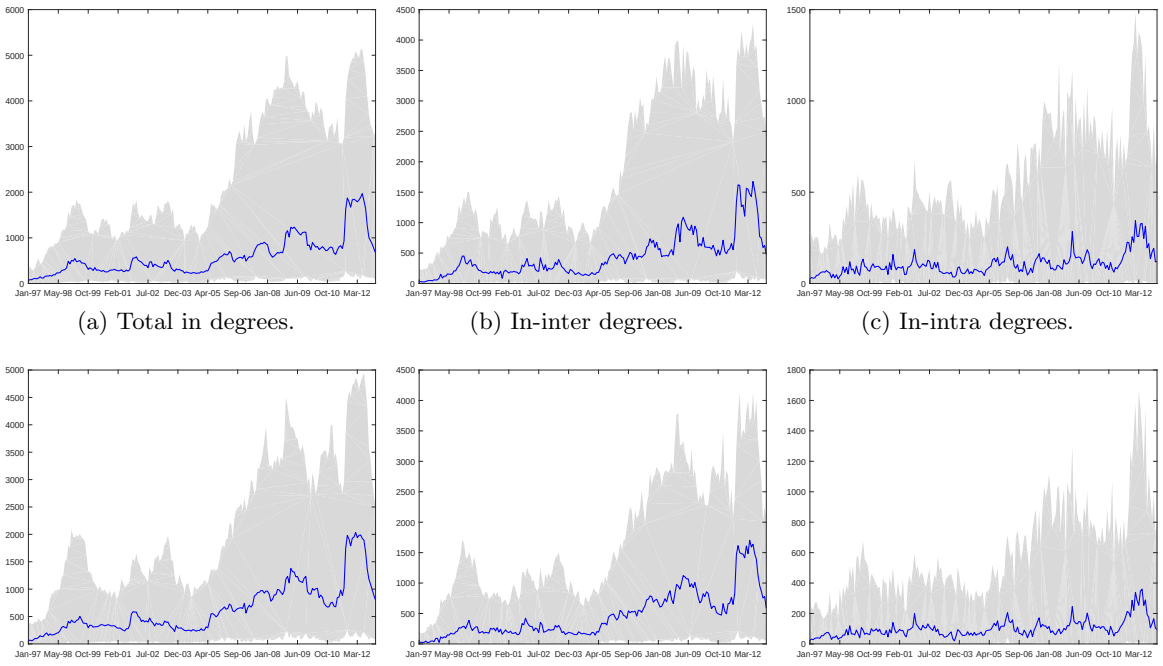

(a) Total in degrees. (b) In-inter degrees. (c) In-intra degrees.

(d) Total out degrees. (e) Out-inter degrees. (f) Out-intra degrees.

Figure 15: 95% high density region (gray area) and the cross-section mean (solid blue line) of total in(out) degrees (first/forth panel), in(out)-inter degrees (second/fifth panel) and in(out)-intra degrees (third/sixth panel) for the European financial network over time.

E Early warning indicator using eigenvector centrality

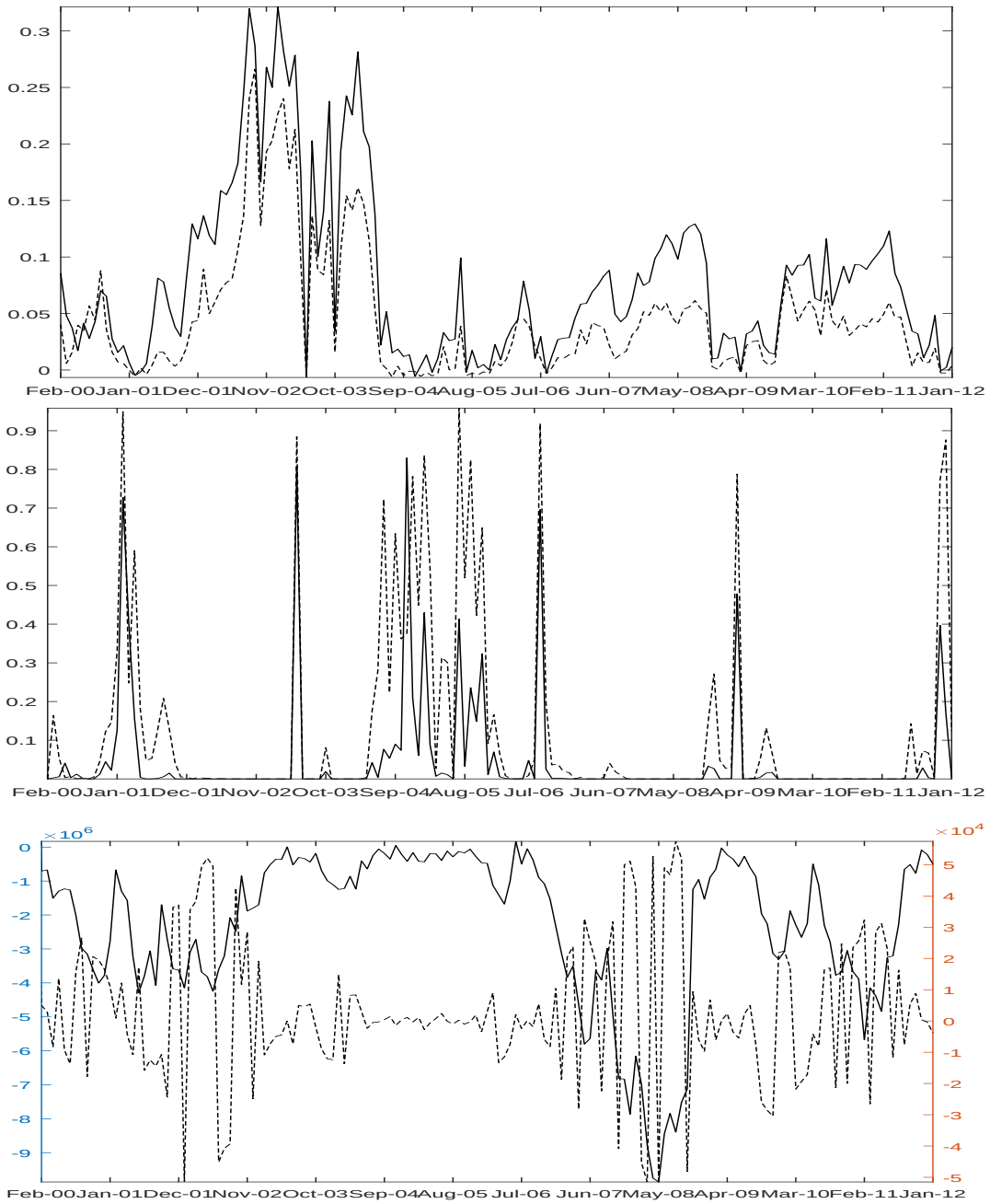

Figure 16: Adjusted R–squared (top), coefficient p-value (mid) and coefficient magnitude (bottom) for the cross-sectional regressions where the dependent variable is the maximum loss incurred by a single institution within the next two years and the independent variable is alternatively the out-inter community degrees (solid line) and the eigenvector centrality (dashed line). See Equation 4.1. Note: The coefficient magnitude are reported on the left y-axis for the out-inter community degrees and on the right y-axis for the eigenvector centrality.

Recent Issues

No. 207	Claes Bäckman, Tobin Hanspal	The Geography of Alternative Work
No. 206	Loriana Pelizzon, Anjan Thakor, Calebe de Roure	P2P Lending versus Banks: Cream Skimming or Bottom Fishing?
No. 205	Horst Entorf, Jia Hou	Financial Education for the Disadvantaged? A Review
No. 204	Loriana Pelizzon, Matteo Sottocornola	The Impact of Monetary Policy Interventions on the Insurance Industry
No. 203	Florian Hett, Felix Schmidt	Pushing Through or Slacking Off? Heterogeneity in the Reaction to Rank Feedback
No. 202	Tobias H. Tröger	Germany's Reluctance to Regulate Related Party Transactions
No. 201	Dirk Krueger, Alexander Ludwig	Optimal Taxes in the OLG Model with Uninsurable Idiosyncratic Income Risk
No. 200	Nils Grevenbrock, Max Groneck, Alexander Ludwig, Alexander Zimper	Cognition, Optimism and the Formation of Age-Dependent Survival Beliefs
No. 199	Tobias H. Tröger	Regulation of Crowdfunding in Germany
No. 198	Henning Hesse, Boris Hofmann, James Weber	The Macroeconomic Effect of Asset Purchases Revisited
No. 197	Benjamin Clapham, Peter Gomber, Martin Haferkorn, Paul Jentsch, Sven Panz	Circuit Breakers – A Survey among International Trading Venues
No. 196	Benjamin Clapham, Peter Gomber, Sven Panz	Coordination of Circuit Breakers? Volume Migration and Volatility Spillover in Fragmented Markets
No. 195	Benjamin Clapham, Peter Gomber, Martin Haferkorn, Sven Panz	Managing Excess Volatility: Design and Effectiveness of Circuit Breakers
No. 194	Baptiste Massenot	A Business Cycle Model with Neuroeconomic Foundations
No. 193	Mario Bellia, Roberto Panzica, Loriana Pelizzon, Tuomas Peltonen	The Demand for Central Clearing: To Clear or Not to Clear, That is the Question